Hindawi Publishing Corporation
Advances in Optical Technologies
Volume 2011, Article ID 628761, 23 pages
doi:10.1155/2011/628761

Review Article

Cavity Solitons in VCSEL Devices

S. Barbay,[1] R. Kuszelewicz,[1] and J. R. Tredicce[2]

[1] *Laboratoire de Photonique et de Nanostructures, CNRS-UPR20, Route de Nozay, 91 460 Marcoussis, France*
[2] *Institut Non Linéaire de Nice, UMR6618 CNRS-Université de Nice Sophia-Antipolis, 1361 Route de Lucioles, 06 560 Valbonne, France*

Correspondence should be addressed to S. Barbay, sylvain.barbay@lpn.cnrs.fr

Received 20 June 2011; Accepted 9 August 2011

Academic Editor: Krassimir Panajotov

We review advances on the experimental study of cavity solitons in VCSELs in the past decade. We emphasize on the design and fabrication of electrically or optically pumped broad-area VCSELs used for CSs formation and review different experimental configurations. Potential applications of CSs in the field of photonics are discussed, in particular the use of CSs for all-optical processing of information and for VCSELs characterization. Prospects on self-localization studies based on vertical cavity devices involving new physical mechanisms are also given.

1. Introduction

In this paper we address experimental results on Cavity Solitons (CS) in VCSEL devices and focus on recent studies and developments. We emphasize on the design and fabrication of electrically or optically pumped broad-area VCSELs used for CS formation and review different experimental configurations. Applications of CS in the field of photonics are discussed, in particular the potential use of CS for all-optical processing of information and for VCSEL characterization. Prospects on self-localization studies based on vertical cavity devices involving new physical mechanisms are also given. The reader interested in the theory of CS formation in semiconductor devices can refer to recent reviews on the subject [1, 2] and also to [3] which provides a general review on CSs and their applications to photonics from a more fundamental viewpoint. A collection of articles on the most recent developments in the field can also be found in [4]. Our goal is to provide a complete and accessible review on past and most recent experimental results on CSs using vertical cavity semiconductor devices, while giving a prospect on future directions.

During the 80s, the main focus of experimental studies on nonlinear dynamics was on temporal dynamics (see, e.g., [5, 6]). Observation of period doubling, quasiperiodicity, intermittency, and chaos in a variety of systems ranging from fluids to chemical reactions appeared in the literature (see, e.g., [7–9]). Optics was not an exception. After the report of period doubling and chaos in a modulated laser [10], several papers showed theoretically and experimentally the appearance of instabilities in optical systems [11]. In particular, laser with injected signal and optical amplifiers have been exhaustively studied [12–17]. Dynamics of semiconductor lasers under injection and delayed optical feedback were also objects of interests mainly because of the possible applications of such devices in optical communication systems [18–20]. Later, mainly during the 90s, the interest shifted towards spatiotemporal instabilities. The possibility of observing optical vortices [21] and finally reach optical turbulence was very attractive, because optical systems were somehow easier to model than hydrodynamical ones. Thus, the comparison between experimental and theoretical results was simpler than in other more complex systems. Several studies reported the appearance of complex spatio-temporal dynamics in optics [22–24] and in particular in laser systems [25–28]. Most of the experiments realized with broad area lasers, thus with a large transverse section or high Fresnel number, showed the appearance of large structures more or less complex but almost always with long correlation length in the transverse plane and, therefore, avoiding the appearance of a complex or turbulent behavior [29]. The reasons for such long correlation order is mainly that it is somehow difficult in lasers to reach a really high Fresnel number, because cavity lengths are usually too long. In

that sense, VCSEL represents an ideal laser to study spatio-temporal dynamics. Effective cavity lengths of the order of $10\,\mu$m, active medium lengths of the order of a quarter-wavelength, almost planar mirrors, and the possibility of having more than $150\,\mu$m in diameter makes this device an ideal candidate to observe structures with very short correlation length and, therefore, complex optical spatio-temporal structures. Several theoretical studies were centered around the formation of patterns in VCSELs [30–32] as well as some experimental ones [33–36].

However, the most interesting results have been obtained in general models of lasers with saturable absorbers [37–39] or optical absorber or amplifier [32, 40, 41]. Numerical and analytical results showed that it is possible to observe localized structures in these optical systems. The main property of a localized structure is that its correlation length is much smaller than the size of the system. Thus, each localized structure will behave as an independent object. In optics, localized structures with a single intensity peak have been called cavity solitons (CSs). Cavity solitons are self-localized states of light appearing in the transverse plane of a cavity as bright spots sitting on a dark background. Experimentally, they can be characterized by the following properties: (1) CSs are self-localized states, independent of the system boundaries whose shape and size is fixed by the system parameters and do not depend on the excitation that gave birth to them; (2) CSs can exist in several (ideally arbitrary) transverse locations of the cavity and can be independently manipulated (written, erased, ...); (3) CS can be "moved" or set into motion. At first sight, they possess characteristics resembling those of self-trapped beams [42] but constrained within a cavity whose propagation path is folded by the cavity mirrors. However, it is worthwhile to notice that single peak localized structures are different from self-trapped beams, because they are created by two fronts connecting two different spatial solutions in a dissipative system. This feature introduces important physical differences; however, that can be fully appreciated only when considering rather subtle theories on CS formation [43, 44]. Some of these physical differences were experimentally observed in a semiconductor-based system in [45]. On the other hand, the presence of a cavity is not necessary either as demonstrated by the observation of single peak localized structures in [46] in a single feedback mirror experiment performed in Na vapour. Thus, CS may be better called single peak localized structure (SPLS), but we will use both names in this review.

CS arise usually under the condition of coexistence of a homogeneous and a patterned stationary state; for the same control parameter values, the solution may approach one or the other state depending upon the initial condition. Localized structures are thus somehow intermediate, controllable states between the homogeneous state and the fully developed pattern. SPLS may also exist in optical systems, where two uniform states coexist, as a result of the locking of two fronts. This mechanism was first studied theoretically and numerically in [47] where self-localized states (then called "diffractive autosolitons") were demonstrated to exist in a nonlinear, bistable, interferometer. Self-localized states were also found in the more general framework of the Swift-Hohenberg equation, a model equation that describes pattern forming systems and applicable in nonlinear optics [39]. The stability conditions for localized structures in 1D were theoretically studied in [43]. The authors then proved theoretically that an infinity of localized structures presenting an arbitrary number of intensity peaks coexist and may be stable for a finite range of parameter values. Later, a similar method was used to study the region of coexistence and the order of the solutions in parameter space [44, 45].

The potential of CSs for applications to parallel information processing was then recognized and demonstrated in [40] and analyzed in the context of a model suited for semiconductor systems in [30]. CS can be excited and erased by a local perturbation at any transverse location of a nonlinear, broad-area cavity and as such play the role of pixels or spatial logical bits. They can be manipulated in phase or intensity gradients, where they can be moved or controlled, a property that relaxes considerably the addressing constrains if one wished to arrange them into 2D matrices.

The main advantages of semiconductor systems over other optical systems, where CS were predicted and observed lie in the fast timescales and small spatial scales associated with CS formation in semiconductor materials. Indeed, the characteristic timescale for CS formation in semiconductor systems is of the order of the carrier recombination time, which is in the nanosecond range, much shorter than other competing macroscopic systems based on photorefractive media [48], liquid crystals [49], or atomic vapors [46] in which CS were also found. Moreover, the characteristic size of a CS is governed by the diffraction length $a \propto \sqrt{L\lambda\mathcal{F}}$, where L is the cavity length, λ the wavelength of light and $\mathcal{F}$ the resonator finesse and is of the order of $10\,\mu$m in microcavities, at least one order of magnitude smaller than in other macroscopic systems. CS necessitate a large and uniform aspect ratio system: a cavity whose transverse extent is much larger than the longitudinal extent such that it can host many transverse modes and allow for spatial decorrelation between different cavity locations. Therefore, broad-area VCSELs appear then as ideal devices to implement CS in semiconductor material systems. The first demonstration of CS in a broad-area VCSEL that stimulated all the ensuing investigations was reported in [50].

This paper is organized as follows. We present in Section 2 the characteristics of broad-area VCSELs with electrical injection and optical pumping designed for CS studies. In Section 3, we then describe experimental results obtained in the amplifying regime, with a cavity driven by an external coherent beam (holding beam). An important new conceptual and applicative step was obtained by the demonstration of a CS laser, that is, a system that does not require a coherent optical injection and emits self-localized microlasers having the properties of the CSs described earlier, as explained in Section 4. Possible applications of CS to photonics are presented in Section 5 with the experimental demonstrations of an optical delay line and of a soliton force microscope. The role of device defects and the applications of CS to device homogeneity characterization are also demonstrated. Finally, new directions in the field of self-localized states using VCSELs are presented in Section 6. We analyze CS

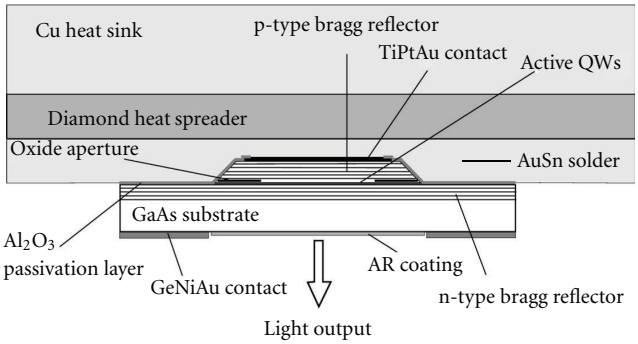

Figure 1: Schematic representation of a broad-area bottom emitter VCSEL structure with diamond heat spreader, after [51] (© 2011 IEEE).

in polarization, Cavity Light Bullets which are 3D-localized states of light traveling in a cavity and CS polaritons which explore new material nonlinearities.

2. VCSEL Fabrication and Design for CS Formation

Broad-area VCSELs play an important role in the development of CS studies in semiconductor systems. However, it was necessary to develop adequate devices, and there were major challenges to deal with, namely, uniformity (concerning pumping and cavity resonance) and thermal management. In the following, we review two solutions that have been proposed and used for CS experimental studies, one with electrical injection and the other with optical injection. The two approaches are presented and the various pros and cons are discussed.

2.1. Electrically Pumped Broad-Area Devices. The bottom emitter VCSEL structure is represented on Figure 1, a detailed description and characterization of which can be found in [51, 52]. The VCSEL is designed for laser operation around 980 nm and optimized for high-power, cw emission. The active zone is composed of three InGaAs/GaAs quantum wells, embedded in an AlGaAs spacer to fabricate the one-wavelength thick cavity. Two high reflectivity $Al_{0.9}Ga_{0.1}As$/GaAs Bragg mirrors close the cavity. The top mirror is p-doped with Carbon, while the back mirror is n-doped with silicon. The back and front mirrors have respectively, 30 and 24.5 pairs of quarter wavelength-thick layers at the targeted cavity resonance of 980 nm. The whole cavity is grown on a GaAs substrate using molecular beam epithaxy (MBE). Circular mesas of diameter ranging from 100 to 250 μm are then etched in the structure before oxidization of the current aperture down to the beginning of the back mirror, where a thin (30 nm) AlAs layer has been included. This layer is oxidized in a water-nitrogen environment at high temperature, leaving an oxidized ring of 25 μm width. A TiPtAu contact is then deposited on top of the mesa and the device is soldered on the heat sink. Heat sinking is provided by metalized diamond sinks soldered with AuSn. On the other side of the VCSEL, the substrate is thinned down to 180 μm and antireflection coated in order to avoid back reflection from the air-semiconductor interface into the gain medium. The diamond can then be attached to a copper submount with a thermal paste. This design ensures a very good overall thermal conductivity of the VCSEL, compulsory for cw operation with large active areas. Cw operation was indeed obtained for 200 μm or even higher diameter VCSELs with very good conversion efficiency and low threshold at room temperature. In [53], the group at the University of Ulm reported room-temperature, cw operation of 320 μm VCSELs in diameter with a maximum output power of 0.89 W and a current density at threshold of 1 kA/cm^2.

This VCSEL design has been successfully employed for the first demonstration of cavity solitons in a semiconductor optical amplifier [50], and subsequent studies on cavity soliton lasers in an extended configuration with a feedback grating [54] or face-to-face configuration [55] (see Section 4).

While a VCSEL possesses in theory a translational symmetry across its useful aperture, this is not the case in practice, and this has important consequences for CS studies. There are indeed two main types of spatial nonuniformities to consider: extended nonuniformities such as those of the cavity resonance wavelength and of the pump, and localized nonuniformities. Because of the growth conditions, layer thicknesses vary over the substrate that results in the appearance of a wedge along a given direction. This wedge does not affect much the spectral characteristics of the Bragg mirrors; however, the gradient in the cavity thickness translates into a cavity resonance wavelength gradient. The effect is all the more important when dealing with broad area devices, because then cavity resonance can vary appreciably across the VCSEL optical aperture. Since CS are sensitive to any parameter gradients [40, 56, 57], this may have major impact on their observation and control. In the seminal experiment on CS in VCSELs [50, 58], a large cavity resonance gradient of 2.34 GHz/μm was measured which prevented the observation of cavity solitons over the entire VCSEL surface. Later, improvements in the growth conditions enhanced the VCSEL uniformity of about one order of magnitude (0.4 GHz/μm [59]) and allowed the manipulation of CS over the whole transverse extent of the VCSEL. As for the pump uniformity, the bottom emitting structure allows to achieve a very good uniformity at the center of the device, whereas the borders suffer the well-known current crowding effect [60]. This manifests itself through the appearance of a high-order flower-like pattern [35] just above the laser threshold and limits the available area for CS manipulation. However, since bottom emitting devices grown on a GaAs substrate are limited to wavelengths above 900 nm to avoid absorption, shorter emission devices may require adopting other techniques. As an example, electrode patterning and use of semitransparent ITO electrodes were considered for the design of 850 nm, broad-area top emitting devices [61] and proved promising for improving electrical injection uniformity of top-emitters. A by-product of this technique would also be the possibility to address CS electrically with local electrodes. Electrode patterning was also used in [62] on a 960 nm top emitting VCSEL in the optical amplifier

regime. Bistability and optical pattern formation which are prerequisites for CS formation were observed. However, the insufficient transverse extension of the VCSEL together with the rather large grid period ($4\,\mu$m) prevented CS formation on a uniformly injected background.

The spatially localized sources of nonuniformity that have also to be taken into account for CS studies are often termed as defects, and may precisely arise from crystallographic defects in the Bragg mirror materials or in the Quantum wells, and lead to CS pinning. More detailed studies on the sample uniformity have been conducted in [63], where CS were used as a spatial probe for defects, and in [64], where localized defects where used as a source of drifting CS. These aspects are detailed in Section 5.2.

2.2. Optically Pumped Broad-Area Devices. An alternative scheme for CS studies relies on the use of optically pumped devices. It may seem at first rather incongruous to deal with optically pumped VCSELs while electrical injection has always represented the ultimate goal in devices. However, the advent of high-power low-cost sources could make it a reasonable choice, all the more that integrated and compact sources can be fabricated. There are several advantages in using optical pumping for CS formation and studies. The first one is that optical pumping allows to easily shape the pump beam using conventional optics and to get rid of current crowding effects by using, for example, a top-hat shape illumination. Since the processing steps after the device growth are reduced, the second advantage one can expect is to reduce the number of defects, and thereby the stress on the final sample, hence the number of pinning sources. The third but not the least advantage is that the pump field may be shaped not only in the transverse but also in the propagation directions, as will be described further in the text and used in Section 4 to design new compact devices. Note also that optical pumping is commonly used in VECSELs for high power lasers [65, 66] and may also be used in the framework of studies on CLB (see Section 6.2). There are, however, problems to be circumvented in order for optical pumping to be a viable solution. The most important problem is the thermal management, to be addressed along its two components: heat production and heat dissipation. It is all the more important here as we consider broad area devices. Heat dissipation is common to the electrical pumping case and the same techniques can be somehow applied. On the converse, heat production is largely specific and depends on the material system considered. In some systems where all the pump power is not absorbed in the gain region, the substrate absorption at the pump wavelength may represent the major part of the heat production. Therefore, a special care has to be taken to avoid it while optimizing the pump absorption in the gain medium. The second contribution to heat production (and to pump energy waste) is the so-called quantum defect, that is, the energy difference between the pump energy and the laser transition (usually close to the bandgap of the semiconductor material). Pump photons absorbed by the semiconductor material produce electron-hole pairs at an energy higher than that of the band gap that cascade to the bottom of the bands through phonon exchange with the crystal lattice (see Figure 2). At the end of the process, all the excess energy is transformed into heat and transferred to the lattice. There is very little to do against this fundamental mechanism except reducing the photon energy excess by choosing a proper wavelength.

As a result, an efficient optical design must minimize heat production and optimize pump absorption into the gain region. Such a design has been proposed in [67] and successfully applied to CS studies in [68] in the AlGaAs material system.

The design relies on the creation of a window at the pump wavelength around 800 nm. The pump window corresponds to a region in the optical spectrum of the cavity where transmission is minimized and pump absorption is maximized, while keeping the cavity properties at the operating wavelength of 870 nm unchanged. This is accomplished by an optimization procedure on the layer thicknesses composing the multilayer mirrors of the cavity. Target values of the transmission, reflection, and absorption spectra in given spectral regions are chosen. The procedure starts with a quarter-wavelength $Al_{0.225}Ga_{0.775}As$/AlAs multilayer stack centered at 870 nm. Then, all the layers composing the back and front multilayer mirrors are allowed to vary in order to reach the desired spectral targets. This is simply done by minimizing an error function that measures the deviation from the ideal target and the actual values, depending on all the layer thicknesses. A Simplex algorithm is used as a minimization algorithm. The algorithm eventually converges towards a set of layer thicknesses values (see Figure 2(b)). As can be readily seen, all the layer thicknesses have different values and the initial periodic structure is lost.

The calculated structure has been grown by metal-organic chemical vapor deposition and the reflectivity and calculated spectra are shown on Figure 3. There is a very good agreement between the calculated and the measured reflectivity spectra. The pump window is easily seen on the left around 800 nm, where absorption is maximized and at the same time pump transmission into the substrate is minimized. The cavity resonance structure at 890 nm is kept. This design ensures that very few pump photons will be absorbed into the substrate and contribute to heating while optimizing the pumping efficiency. The width of the pump window is 20 nm which introduces immunity against eventual temperature induced shifts of the reflectivity spectra through temperature-induced index change and subsequent dramatic effects on the pumping level. It also allows pumping with a large numerical aperture microscope objective or lens. The VCSEL can then be processed with other techniques to enhance heat removal, such as substrate removal and replacement with a high thermal conductivity substrate such as SiC substrate or diamond substrate. Note that this technique does not prevents heat absorption into the substrate, since, in general, the bonding layers absorb very efficiently the pump photons. Substrate removal and SiC bonding with Ti-InAu bonding has been employed in the sample used in [68].

The same design technique has been used and refined to fabricate a monolithic VCSEL with intracavity saturable absorber. VCSELs with intracavity saturable absorbers were

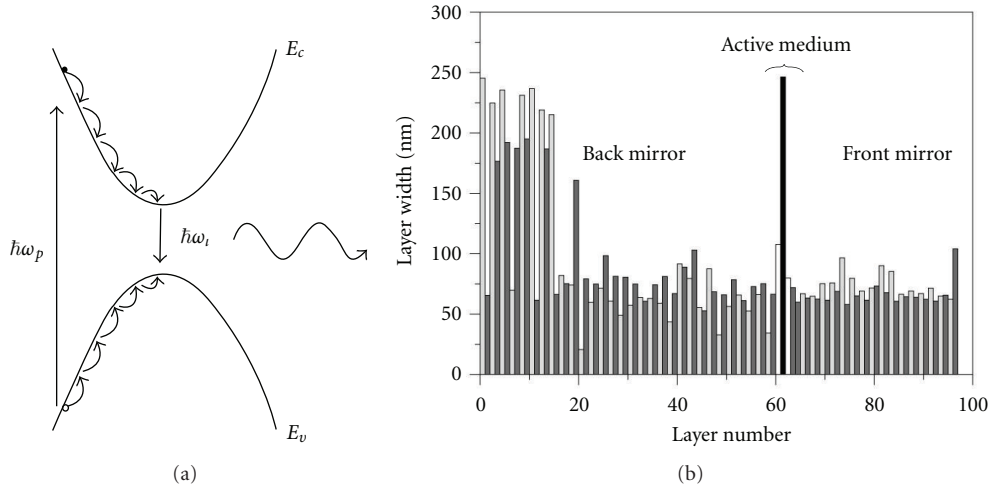

Figure 2: (a) Schematic representation of optical pumping in a semiconductor material: a pump photon of energy $\hbar\omega_p$ is absorbed in the semiconductor material creating an electron-hole pair. The electron and hole cascade to the bottom of the bands releasing extra energy to the lattice and eventually recombine either radiatively or nonradiatively. (b) (after [67]): Layer widths of the optimized structure. The substrate is on the left side of the figure. The cavity is filled by two absorbing $Al_{0.07}Ga_{0.93}As$ spacers (layers 61 and 63) white bars around a bulk GaAs active layer (layer 62, in black). The back and front Bragg mirrors are composed of alternating $Al_{0.22}Ga_{0.78}As$ (dark gray) and AlAs (light gray) layers.

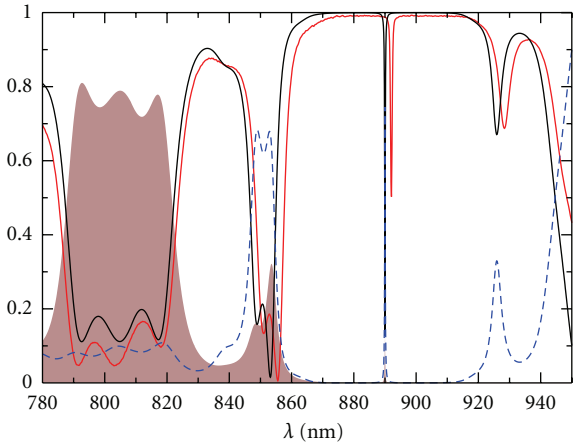

Figure 3: Calculated and measured spectra of the optimized cavity. Red line: experimental reflectivity spectra. Black line: corresponding calculated reflectivity spectrum. Brown: calculated absorption. Dashed blue: calculated cavity transmission.

already considered in the prospect of building self-pulsing or bistable vertical-cavity lasers. Several designs have been proposed for electrically injected devices. A quantum well may for example be placed in the upper or lower mirror stack with a shorter carrier lifetime [69] or with an additional contact for controllable operation [70]. Self-pulsing have also been observed in small area, oxyde-confined VCSELs thanks to the difference between the carrier and the optical mode confinement [71]. A double cavity may also be used for controllable self-pulsing or bistable operation [72]. These techniques necessitate either a small area cavity, a fast saturable absorber, or a complex electrical design and are not suited for CS studies. An original design for a vertical cavity laser with intracavity saturable absorber has been proposed in [73]. Using the same technique as explained before, a cavity having a saturable absorber section and a gain section is designed. The gain region has two InGaAs/GaAs QW for lasing around 980 nm. The saturable absorber section has one InGaAs/AlGaAs QW. All the QWs are placed at the antinode of the resonant cavity field targeted at 980 nm. The cavity is designed for optimized optical pumping around 800 nm. Therefore, in addition to the previous optimizations, the multilayer mirror widths have also to be calculated in order to satisfy a condition on the pump field intensity inside the active zone of the cavity. The pump field in almost zero in the whole pump window at the location of the SA QW. The gain QW barriers absorb the 800 nm pump field, whereas the SA QW barriers are made transparent to the pump wavelength in the pumping window by aluminium incorporation inside the barriers. The design is depicted in Figure 4 and has been successfully used to demonstrate bistability, self-pulsing, and a compact cavity soliton laser (see Section 4).

3. CS in Semiconductor Optical Amplifiers

The most studied system in optics is represented in Figure 5. A nonlinear medium inside an optical cavity is driven by a homogeneous optical beam covering the whole transverse section of the device. The system can be set such that the output intensity is zero and all the incoming beam is absorbed by the saturable medium. If the condition for the bistable behavior is fulfilled, then a short and narrow optical pulse may ignite a small region of the device. Such an optical pulse is called the writing beam. If it is in phase with the holding beam, a CS is created at the location where it impinges that persists after the writing pulse disappears. In a similar

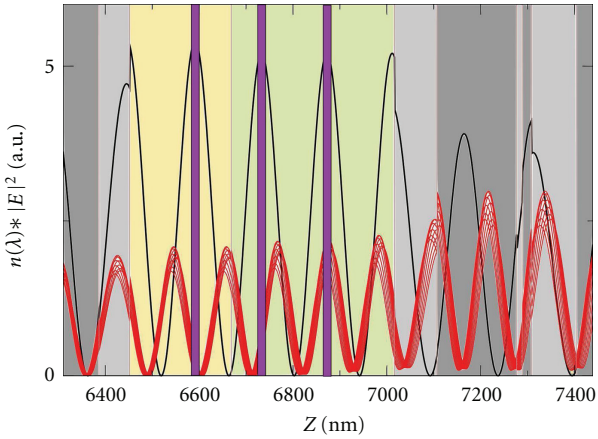

Figure 4: Active zone of the VCSEL-SA and field intensities at the cavity resonance (black, divided by 400) and at the pump wavelengths (in red, between 795 nm and 805 nm) versus the growth depth. The active zone is composed of two regions (in yellow and green): the SA region (yellow) with one InGaAs/$Al_{0.22}Ga_{0.78}As$ quantum well and the amplifying region (green) with two InGaAs/$Al_{0.05}Ga_{0.95}As$ quantum wells. The first few layers composing the the front and back mirrors is visible on the right and left respectively. of the active zone. Light grey: AlAs. Dark grey: $Al_{0.22}Ga_{78}As$. Note that the SA quantum well is at a node of the pump fields in the whole range of possible pump wavelength while being at an antinode of the field at cavity resonance. After [73].

way, another CS can be created in any other location provided the correlation length of the localized structure is significantly smaller than the transverse size of the device. CS written in the way described above can be erased by sending a pulse quite similarly to the writing pulse at the same location but with phase opposite to that the holding beam.

Experimentally, CS have been observed in several systems based on photorefractive crystals [48], Na vapors [46], liquid crystal light valves [49, 74], semiconductor optical amplifiers [50, 68], and lasers [54, 55, 73, 75]. In the latter, most experiments have been done in VCSELs, because their short cavity and large diameter insure a Fresnel number large enough to avoid the formation of patterns correlated over the whole extension of the system. CS have been observed in amplifiers both electrically [50] and optically pumped [68]. The pumping rate was set high enough to provide gain in the active medium but low enough to maintain the VCSEL below the laser threshold. However, it must be noted that similar results have been obtained with an injected VCSEL pumped slightly above threshold [59].

A typical experimental setup is shown in Figure 5. A bottom emitter VCSEL with a diameter of 150 μm was injected by a coherent optical beam produced by an edge emitter laser with an external cavity in a Littrow configuration. Thus, the holding beam can be fine tuned in the range 960–980 nm. This beam was spatially filtered such that the intensity could be considered as almost uniform across the whole section of the VCSEL, and thus not introducing an additional gradient component. The holding beam power was controlled by an acousto-optic modulator together with a polarizer. The second output coming from the external cavity laser was then used as a coherent writing beam (WB). This beam was prepared so as to obtain a 10 μm waist; its power was controlled by an acousto-optic modulator. The phase relation between the writing beam and the holding beam was controlled by piezo-positioning a mirror on its own path. The reflected output of the VCSEL was monitored globally by a CCD camera or locally using a fast photodetector.

The observation of CS in an electrically pumped VCSEL amplifier [50, 58] and the demonstration of their mutual independence is explained in Figure 6. Similar results have been obtained in optically pumped VCSEL amplifiers [68]. The demonstration relies on the independent writing and erasure of two CS at two different locations of the VCSEL. In the first demonstrations, the locations where the independent manipulation of the CS could be obtained in practice were limited by the presence of a strong cavity resonance gradient. In the following experiments, new devices with much smaller gradients were provided and allowed manipulation over almost the whole transverse extent of the device, that is, 200 μm. The switching characteristics were analyzed in [76]. A sequence of independent control of two CSs using in-phase local excitation with the holding beam (writing beam) or π-phase shifted beam (erasure beam) is shown in Figure 6.

The use of the phase parameter to control the writing or erasure process of a CS reveals in fact quite cumbersome in practical applications. However, an incoherent switching technique has been demonstrated by Barbay et al. in [68]. Using a specially designed optically pumped VCSOA as described earlier, they have shown that CS writing and erasure can be achieved by short pulses (60 ps duration), at a wavelength far from that of the holding beam, demonstrating a mechanism free of phase relationship. This technique relies on the observation that CS in semiconductor devices are compound objects. While a localized structure is formed in the intracavity field distribution, a counterpart forms in the carrier density. Hence, it is possible to excite CS by locally adding carriers. The fact that both writing and erasure are possible by local carrier injection, with slightly different HB parameters though, is intriguing and has been explained in terms of local temperature effects in [77]. As in the coherent case however, a delay is observed in the writing process which depends on the operating conditions and which is of the order of 100–200 ns (against several ns in the coherent case). The erasure process is faster and occurs without delay in a timescale of a few ns or less. The writing delay can be reduced by increasing the writing power.

In theory, one needs a translationally invariant system for CS formation and control. In practice, the presence of gradients in the system is unavoidable. They arise from different sources.

(i) Device growth and fabrication: the VCSEL cavity resonance used in [50] had a linear variation along one diameter of the device. This variation creates a linear gradient of one of the most important control parameters in the experiment: the detuning between the cavity resonance frequency and the frequency of the holding beam. Though generating important

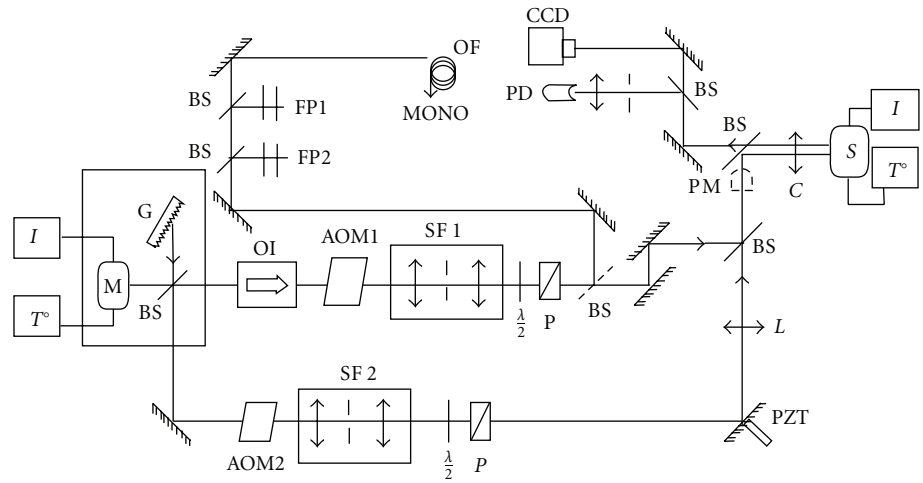

Figure 5: Experimental setup. M, high power edge emitter laser; I, current driver stabilized up to 0.01 mA; TO, temperature controller; G, grating; OI, optical diode; FP, Fabry-Perot resonators; AOM, Acousto-optic modulators; SF1, beam expander configurator with spatial filtering; SF2, beam reducer configurator with spatial filtering; S, broad-area vertical cavity surface emitting laser; C, collimator; CCD, camera; PD, Photodetector; PZT, piezoelectric ceramic; M and BS, mirrors and beam splitters; PM, power meter (optional); $\lambda/4$, $\lambda/2$ wave plates; P, polarizers; OF and MONO, optical fiber and monochromator.

consequences, it can be controlled by the growth conditions.

(ii) Nonuniform distributions of carrier injection in electrically injected devices. Usually, electrically pumped broad area devices present a current density higher at the borders than in the center of the active zone (current crowding effect). For this reason, a bottom emitter structure was preferred in the first demonstration of the generation of localized structures in a VCSEL because the longer distance between the ring electrode and the active medium translates into a more uniform current distribution.

(iii) Misalignment of the holding beam with respect to the optical axis of the VCSEL.

(iv) Not completely uniform intensity distribution of the holding beam.

(v) Defects in the VCSEL structure. Some defects may repel the localized structure while others tend to pin them (see Section 5.2).

All these gradients could affect the generation and the stability of CSs. Localized structures move under the effect of a gradient and in semiconductor devices can move fast enough to prevent a CDD camera from detecting them. Fortunately, some defects or unwanted gradients of the device or induced by the imperfections in the experiment would pin them so that they remain stable and steady. During the first experiments, CS appeared always at the same set of positions. The introduction of external intensity or phase gradients allowed to move them around in a controllable way demonstrating the independence from the boundaries and the possibility to observe them in the whole transverse plane of the device which can be relevant for some applications as we will explain in Section 5.

Later, cavity solitons have been observed in electrically pumped VCSEL above threshold (see Section 4). The main properties of localized structures in optical amplifiers are the intensity and phase stability. The good stability in intensity is defined by the fact that the low and high intensity of the bistable cycle are very well defined at all positions and remain the same as much as the parameters are kept constant over the whole transverse section of the device. If the optically injected VCSEL is driven above threshold instead, the lower branch of the bistable cycle is usually unstable and the CS intensity fluctuates in time. The holding beam defines the phase of the CS so that the phase is fixed all across the transverse section of the device. Thus, a possible transverse phase wave generated by the fast change in intensity at the position of the CS will not propagate. If a phase wave is created, then it will act as a phase gradient for a second CS and it will move towards the border of the device as explained in [78].

In all cases, the experimental results have been compared with numerical ones showing very good qualitative agreement and in some cases even quantitative agreement with semiclassical models.

4. CS Lasers

Vertical cavity semiconductor optical amplifiers (VCSOAs) allowed to demonstrate many useful properties of CS for possible applications to all-optical processing of information (see Section 5). However, they necessitate the use of a coherent holding beam for optical injection which makes the experimental implementation more difficult, bulky, and costly. Moreover, CSs in such a case sit on a nonzero background and the contrast between the CS peak intensity and the background intensity is reduced. This is why laser CS would be needed to circumvent all these problems.

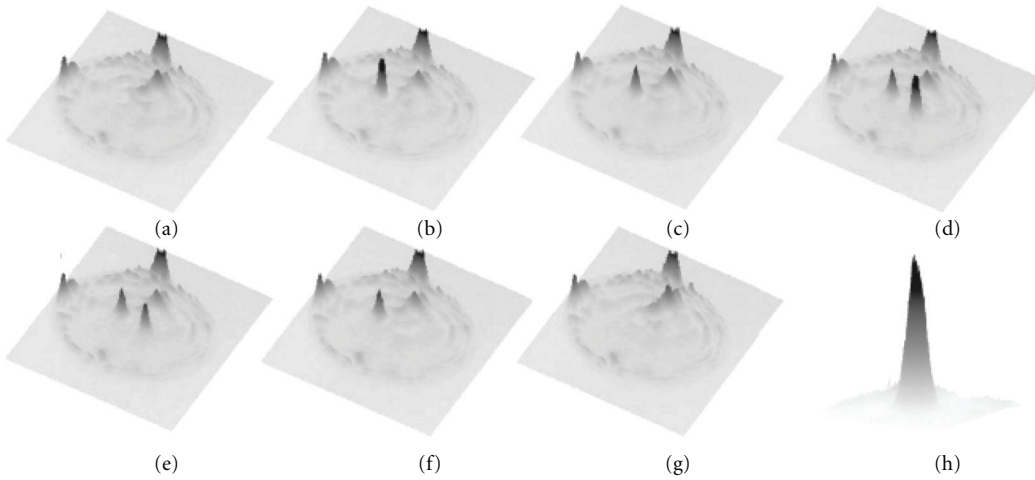

Figure 6: 3D representation of the VCSOA near-field intensity distribution, after [58]. The holding beam is always on, and all parameters are kept constant in the sequence (a)–(g). (a) The writing beam (WB) is off; (b) the WB induces the appearance of a single CS; (c) the WB is off again, and the CS remains; (d) the WB is displaced in position, and switched-on again and generates a second CS; (e) the WB is off again and the two bright spots coexist; (f) the WB targets the second CS, but the relative phase of WB with respect to HB has been changed, and the CS is erased; (g) the WB targets the first CS, and it is erased in the same manner as in (f). Once the WB is blocked, the intensity distribution is identical to (a). In (h) is shown the CS profile.

It is to be noted that contrarily to what was believed at the early stages of their studies, CS in the laser regime can indeed exist in a VCSOA. As a laser with injected signal is known to develop temporal (Hopf) instabilities that can couple to the spatial degrees of freedom and drive the system to a regime of spatio-temporal chaos, this seemed *a priori* not favorable to the formation of CS which require a stable background to form on. It was nevertheless shown in [59], both experimentally and theoretically, that CS can be observed in a driven VCSEL above threshold. The theoretical modeling indicate that CS can exist even on the oscillatory background generated by the onset of a Hopf instability. This is confirmed in the experiment, where it is shown that CS can survive in a narrow parameter range. Still, the laser CS thus obtained is limited by the necessity of a coherent holding beam (HB), which in addition to injecting energy, fixes the phase of the CS. This is in contrast to the case of a true, "free-running" CS laser (CSL) which can be described as a self-confined microlaser for which the phase is not fixed. This last point has important consequences regarding CS interactions.

Theoretically, CSL have been found in two-photon active media [79] or in dense two-level systems [80]. In the context of semiconductor CSLs, two possible bistable laser schemes have been studied. The first one is the VCSEL with frequency selective feedback, which led also to the first demonstration of CSL in a semiconductor system [54], and the second one is the VCSEL with saturable absorber, studied in a compact and an extended cavity configuration.

The VCSEL with a frequency selective feedback scheme is depicted in Figure 7. A broad area VCSEL of 200 μm diameter emitting around 980 nm is used in an external cavity configuration where a grating in Littrow configuration here, or a volume Bragg grating in later experiments, is used to close the cavity. A pair of lenses is inserted inside the cavity in the self-imaging configuration in order to keep a high Fresnel number cavity hence the possibility to have a high number of transverse modes and allow for spatial decorrelation. A half-wave plate is used to match the VCSEL polarization direction of the laser emission to those of the beam splitters—BS1 and BS2—and of the grating. The grating is tuned such that its maximum reflection is red detuned with respect to the VCSEL longitudinal mode. Above a certain threshold in the injected current (lower than the solitary laser threshold), the system starts to emit and displays several isolated spots whose characteristics are those of a CSL [54]. The spots are bistable, almost identical in shape and size (10 μm), individually controllable in certain transverse locations of the laser (see Figure 7(b)), and can be put into motion or "dragged" by an appropriate intensity gradient obtained by inserting a comb filter in the cavity. The emission spectrum of each spot is narrow as expected in a laser. The writing beam that provides a temporary and localized excitation is not coherent with the spots. Further details on the different switching techniques are described in [81], and a model that qualitatively agrees very well with the observations is proposed in [82]. Interestingly, the switch-on and off are obtained with an incoherent beam and the function (writing or erasure) is controlled by the position of the localized excitation with respect to CSL location. This position depends on the grating orientation. The minimum writing beam pulse width needed to ignite a CSL is below 15 ns (lower limit not known due to experimental limitations), while the shorter the writing beam pulse, the higher the intensity is required [83]. Spontaneous switch is also observed following an uncontrolled perturbation (being of mechanical, thermal, optical origin). In such a case, the switch on is accompanied by short transient pulses, a feature of interest with respect to Section 6.2. Multipeak structures are also observed [84] and

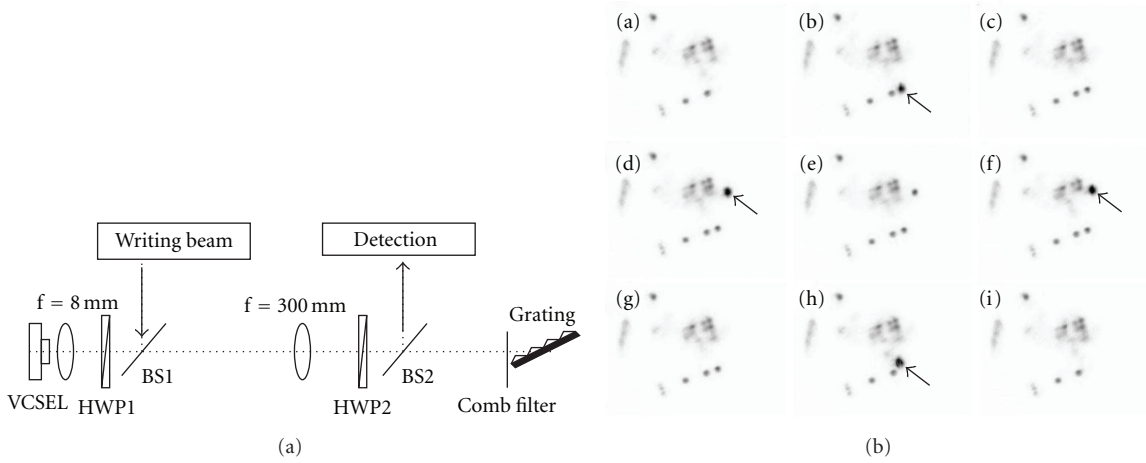

Figure 7: (a) Experimental setup of a CSL consisting in a VCSEL with frequency selective feedback. One pair of lenses are inserted inside the cavity in the self-imaging configuration. Beam splitters BS1 and BS2 are used for writing beam input port and for output detection. (b) Sequence of images (inverted contrast) of the VCSEL surface showing the independent writing and erasure of two CSL. Reprinted with permission from [54]. (© 2011) by the American Physical Society.

associated with a CS-splitting phenomenon reminiscent of the homoclinic snaking curve observed in amplifier systems [45].

It has been long known that semiconductor lasers with saturable absorbers can be bistable. They constitute thus the second system of choice for CSL studies. The first demonstration of a CSL with a saturable absorber has been reported in [55]. The experimental setup consists of two mutually coupled, face-to-face, VCSELs depicted in Figure 8. It is composed of two broad area (200 μm diameter) 980 nm VCSELs, provided by the same company (ULM Photonics) as in the previous demonstration. The VCSELs are optically coupled by lenses in the self-imaging configuration. A beam splitter is used for detection and for localized excitation. One VCSEL is biased above transparency and operated in the gain regime, while the other VCSEL is biased below transparency and operates in the saturable absorption regime. The temperature of the gain VCSEL is set such that its emission is slightly (1 nm) blue detuned with respect to the below-threshold spontaneous emission of the second VCSEL. The output detected when the gain laser current is varied is shown in Figure 8. For low currents, light emitted by the gain device is almost fully reflected by the second VCSEL because of the frequency mismatch. The system starts to lase with a threshold lower than that of the solitary laser (Figures 8(a) and 8(b)). When laser emission starts to saturate with increasing current, and because of its thermal red-shift, laser emission starts to decrease as its coupling with the second VCSEL progressively increases. When enough intensity can enter the saturable-absorber cavity, absorption saturation takes place, and a bistable characteristics is locally recorded. In the near-field image of the sample, bistable laser spots appear that can be controlled independently with an external beam. Here, a localized excitation whose wavelength is close to that of the emitted light is used. The switching process is analyzed in [85]. Switch-on is accompanied by rather long (600 ns) transients composed of 150 ps pulses with a period equal to the round-trip time of the external cavity, relevant in the context of Section 6.2. Multistability among several, multicolored monochromatic CSL is analyzed and modeled in [86, 87]. The proposed model also explains the observation and control of bistable laser vortices reported in [88], that were predicted earlier in wide-aperture, class-A lasers with saturable absorption in [89].

A compact CSL has been demonstrated in [73, 75]. The device, a monolithic, optically pumped, vertical cavity laser with intracavity saturable absorber, is described in Section 2.2. At difference with the previous demonstrations, this system is purely single-longitudinal mode. Its theoretical description is intrinsically simpler and laser CS models have been studied in [90, 91] and in [92–94] for semiconductor laser models (see also [2] for a recent theoretical review). The vertical-cavity is optically pumped uniformly on a 70 μm diameter.

Fast and sequential independent and incoherent writing/erasure are demonstrated with short (60 ps) pulses at a maximum rate of 82 MHz (see Figure 9). Note that the switch-on time is very fast (several ns) and only limited by relaxation oscillations [75], while the switch-off time is of the order of 1 or 2 ns, as expected in this kind of systems [95]. The same beam characteristics were used for both switch-on and switch-off. Theoretical work [95] suggests the important role played by the writing/erasure beam width in the spatiotemporal dynamics that may explain why the same intensity distribution can allow exciting or erasing a laser CS.

One important point in CSL with respect to CS in amplifying systems is that the phase of the localized state is not fixed and may have *a priori* arbitrary value. Nevertheless, the phase profile of a laser CS is larger than its intensity profile, and it was shown in [94] that CSLs at a distance shorter than 60 μm will interact and form a cluster. The practical value in experimental systems above which LCS may be independent is however, smaller because of system's inhomogeneities that destroy the long-range interactions. If the distance between

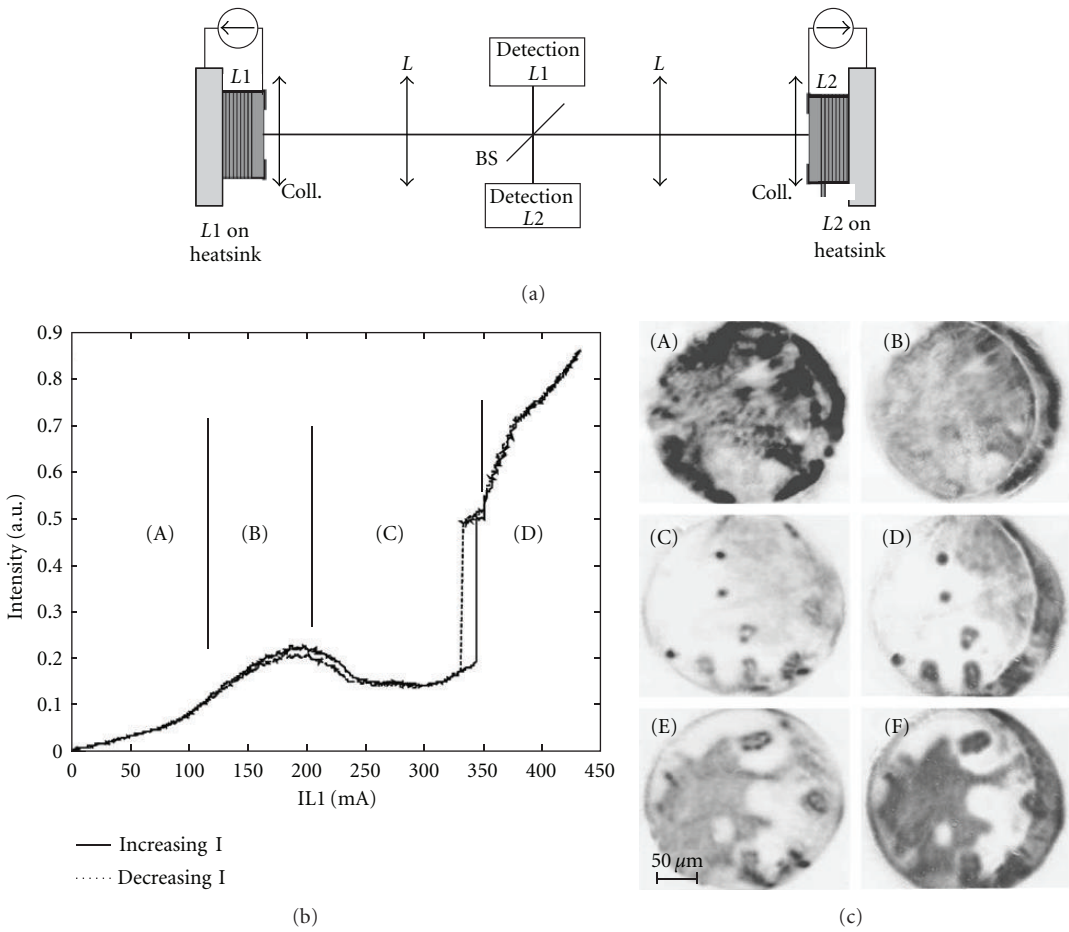

Figure 8: Experimental setup (a) and experimental results (b) and (c) obtained in the face-to-face VCSELs configuration (see text for details). Reprinted with permission from [55]. (© 2011) by the American Physical Society.

each laser CS is too small then laser CS shall not be independently controllable anymore [75]. The properties of clusters of laser localized structures and the associated motion is thoroughly studied in the theoretical paper of [96, 97]. Experimentally, clusters arise either spontaneously [75] or following a "splitting" process as the pump is increased as in [84, 98]. An experimental confirmation that uncoupled, single-peaked Laser CS are mutually incoherent is given in [84, 98], while clusters are found to have a well-defined phase relationship as reported in [98].

An important feature of CSL not yet clearly experimentally demonstrated is related to the control of their motion. In amplifying systems, motion can be induced either by a phase or intensity mask on the holding beam (see Section 5). In laser systems, one cannot use the phase degree of freedom anymore. Motion can be induced by instabilities, as studied in [99, 100], where spontaneous motion is expected when the ratio of the carrier lifetimes in the active and passive medium, respectively, is below a critical value. If boundaries are included, for example, circular boundaries, CS move along the boundaries, an effect that can be exploited for an optical clock [100]. Experimentally, techniques to control the index of refraction of the cavity by using a spatial light modulator [101] may prove interesting, at the expense of a greater complexity of the experimental setup. Controlling the CSL motion remains therefore an important challenge.

5. Applications of CS to Photonics

The main properties of localized structures or cavity solitons in optical systems are twofold (1) They can be switched-on and off independently so that one can control their appearance and disappearance. (2) If the system is homogeneous in the transverse plane, CSs are free to move, thus they will feel the existence of any gradient. In other words, their position and their velocity can be controlled by adjusting a gradient of intensity and/or phase. These properties raise the idea that one can use localized structures in applications related to information processing. The most natural one is an all optical memory [38, 40, 50, 102, 103] due to the controllability in position and switching capabilities of CSs. However, there are several other possible applications not so obvious at first sight. In the following, we present two possible applications of cavity solitons: one in the optical information processing context, an all optical delay line; and

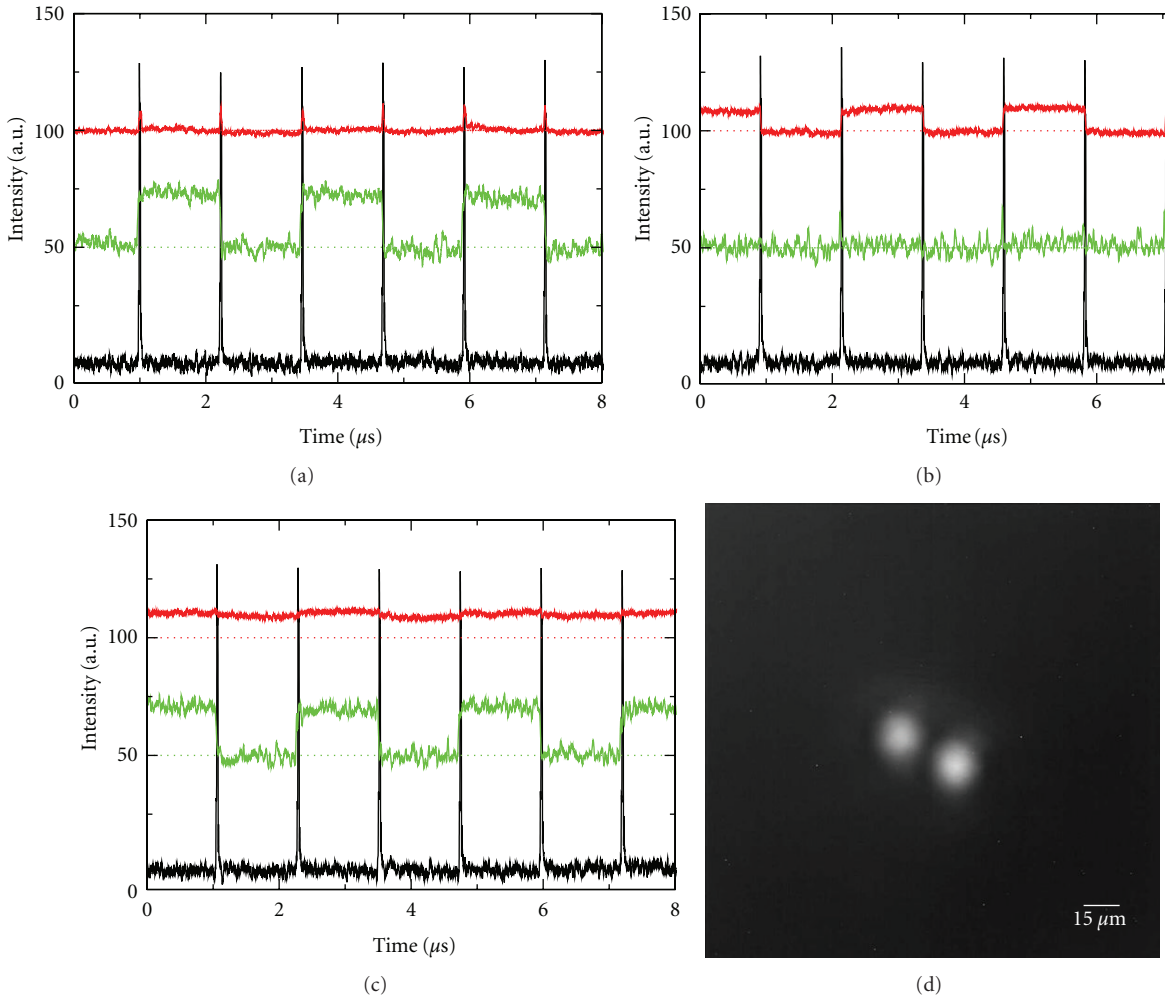

FIGURE 9: Independent and sequential writing-erasure of one cavity soliton while keeping the neighboring cavity soliton unchanged (a,b,c). The black trace corresponds to the incoming localized excitation pulse, and the middle (upper resp.) trace, green (red resp.) online, corresponds to the leftmost (rightmost resp.) cavity soliton. The zero intensity levels of the upper and middle traces (dashed lines) have been artificially offset by 100 and 50, respectively for clarity. An averaged image of the two-cavity solitons considered is shown in (d). After [73].

another for material structure determination: a soliton force microscope.

5.1. All-Optical Delay Line. Apart from the existing electronic devices that are used today as shift registers, there has been increasing interest in all optical delay lines in the last few years. Most of the proposed all-optical systems are based on slowing down light by modifying the group velocity. Such variation can be a consequence of a nonlinear process like electromagnetically induced transparency (EIT), stimulated Brillouin scattering (SBS), and so forth. In [104–108], it is possible to find several schemes based on slow-light in order to realize a delay line (Figure 10).

Using localized structures, it is possible to propose a completely different approach based on injecting a stream of optical pulses into a nonlinear device. Each injected pulse will create a CS. If a linear gradient is somehow superimposed, the CS will drift along this line at a speed which, for some range of parameter values, is proportional to the gradient. The CS can be recovered later at a different spatial position. This method was proposed for the first time by Firth and Scroggie in 1996 [40, 57] and demonstrated experimentally in Na vapors by Schäpers et al. in 2001 [109] and by Pedaci et al. in 2008 in a VCSEL [110].

The optical system used in [110] is a bottom emitter VCSEL as described in Section 2.1. The broad area device (200 microns in diameter) is injected by a collimated beam focused by a cylindrical lens. This allows the generation of a homogeneous injection beam along a line transverse to the direction of propagation of light on the microresonator. The intensity of the injected field, the detuning between the cavity resonance and the injected field frequencies, and the pumping current of the VCSEL were set at typical values for which the CS may exist in such devices (see [58]). Five fast avalanche photodiode detectors are placed in the near-field image plane so as to detect the output intensity of the device

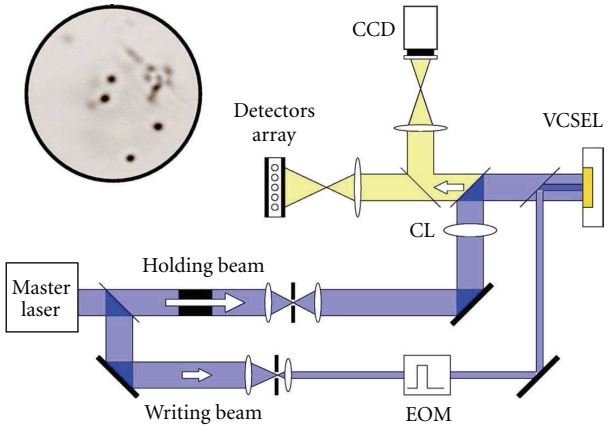

Figure 10: Experimental setup. Vertical cavity surface emitting laser (VCSEL); cylindrical lens (CL); electro-optic modulator (EOM); tunable master laser (ML). Inset: transverse profile emission (negative image) of a 200 μm section VCSEL, in the regime of CS existence under injection by a broad holding beam. Four CSs are present in the image. (figure reproduced from [110]).

along the line defined by the holding beam. A linear phase gradient is generated by tilting the holding beam with respect to the axis normal to the VCSEL. The amount of gradient is then controlled by the angle of incidence of the holding beam. A CS is then created by applying a 100 ns writing beam pulse at some point of the microresonator. This CS drifts as a consequence of the presence of a phase gradient along the line defined by the cylindrical lens and its passage is detected by the fast photodiodes. The detected output intensity as a function of time is displaced depending on the detector considered, as can be seen in Figure 11. It is clear then that the CS generated at one point in the transverse section of the device is drifting along a line and detected sequentially by the five fast detectors. Knowing the distance between the corresponding points detected by the fast photodiodes (7 μm), the speed of the CS is measured as a function of the tilt-induced phase gradient. In the case represented in Figure 11, the average speed of the CS is 4.7 μm/ns. The observation provides a proof-of-principle for an all optical delay line based on the property of motion of the CS under the influence of a phase gradient.

The experimental results obtained in [110] are in good agreement with numerical ones obtained by integration of a semiclassical model. In Figure 12, numerical results are shown corresponding to the speed of CS as a function of the gradient strength which are compatible with the experimental ones. For a large interval of the gradient strength, the velocity of the CS is almost linear and can be easily controlled between 1 and 4 micrometer/ns. This is much smaller than those obtained on the devices based on slowing down the speed of light by changing the index of refraction of the medium. Furthermore, those theoretical results indicate that the speed of the CS can be increased by increasing the decay rate γ of the carrier density in the semiconductor device (Figure 12(b)). The system proposed in [110] provides not only an operation of the device as an all optical delay line but also an all optical pulse reshaping of the incoming optical pulse. Amplitude fluctuations of the incoming pulse are eliminated because of the threshold response of the medium to generate a CS. This functionality may be very useful in order to avoid deterioration of the transmitted signal.

5.2. Soliton-Force Microscope/Role of Defects. As stated before the position of a CS or localized structure can be controlled by a gradient. In [103], it was shown that it is possible to position the CS at the maximum of an intensity or phase gradient. On the other hand, CS can be pinned by defects in the structure of the device. The defects act by generating a gradient. If all other parameters are considered uniform, only the gradients generated by the defects will determine the final position of the CS. One may distinguish between two types of defects: those that are able to pin the CS and those that repel them. Thus, in presence of gradients of different origins, the stable positions of CSs will be those where the forces applied on them compensate. This view may however, be mitigated by the recent theoretical demonstration in [111] that CS may also feel the boundaries, even if they are far from them, so that only a finite set of positions are allowed. This point lacks; however, a clear experimental demonstration.

In [63], it was proposed to monitor the motion of CS under the effects of externally applied gradients. Deviation of the CS trajectory from the one imposed by external gradient reflects the presence of a defect of the structure revealing its attractive or repulsive character. As a consequence, a map of the inhomogeneities of the device is given by the frequency of visits of the areas of the device when the motion of CSs is imposed across the entire section of the system.

The experimental setup used in [63] to record the map of inhomogeneities is similar to the one described in the previous section. The motion of the CS is induced by creating a gradient in the transverse direction to the propagation of light. In particular, a spatial modulation of the holding beam intensity was introduced. In order to control the gradient strength and position of the intensity maxima a Mach-Zender interferometer was inserted in the path of the holding beam. The interferometer is set to generate an intensity profile on the VCSEL formed by fringes of 10 μm size. The pattern allows confining the position of CSs along the direction perpendicular to the fringe. No gradient is present in principle along each interference fringe. In such conditions, only the imposed intensity gradient or intrinsic gradients in the device can induce a motion of the CS. The fringes are adiabatically shifted horizontally by just moving a mirror of the Mach-Zender interferometer controlled by a PZT ceramics. The CS is expected to be dragged in a straight line while the fringe is moved, but it was observed that it deviates from this line. The deviation is attributed to the presence of internal gradients generated by defects in the device. The procedure was repeated for different orientation of the fringes. For an ideal defect-free medium, such analysis would result in a uniformly gray map. As long as inhomogeneities are present, some regions are visited very often by the CS while others are almost never visited. Thus, high-intensity regions in the map correspond to attractive defects while

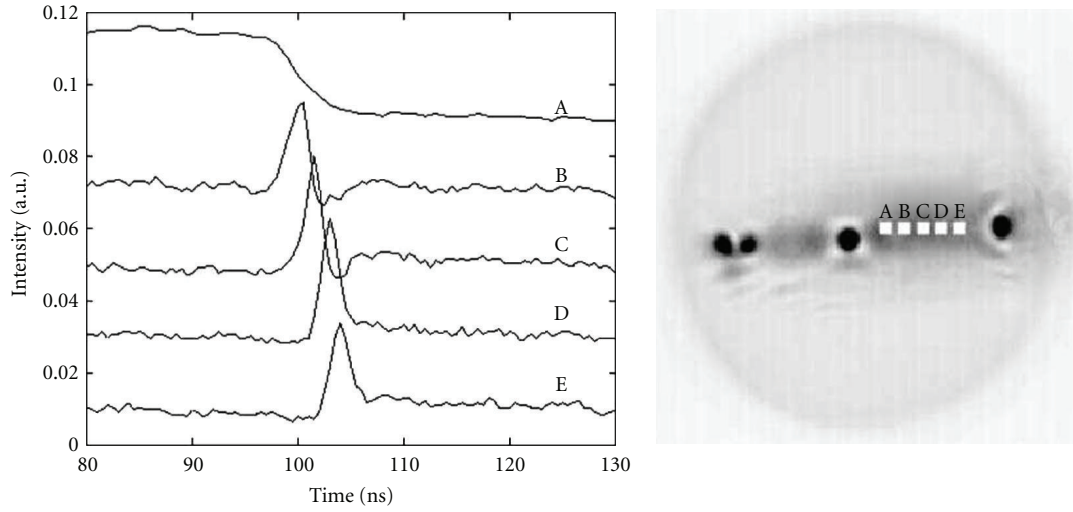

(a) (b)

Figure 11: Passage of a CS in front of a linear array of five detectors (A)–(E). (a) Time traces of these detectors, displaced vertically by 0.02 units for clarity. Detector A monitors the point addressed by the writing beam, applied at time $t = 0$. (b) Positions of the detectors in the transverse plane (indicated by squares). The area monitored by each detector has a diameter of less than 7.2 μm and the separation between neighboring detectors is 8.9 μm. Also shown is a time-averaged output image of the VCSEL during the CS drift (charge coupled device camera exposure time of about 1 ms). Figure reproduced from [110].

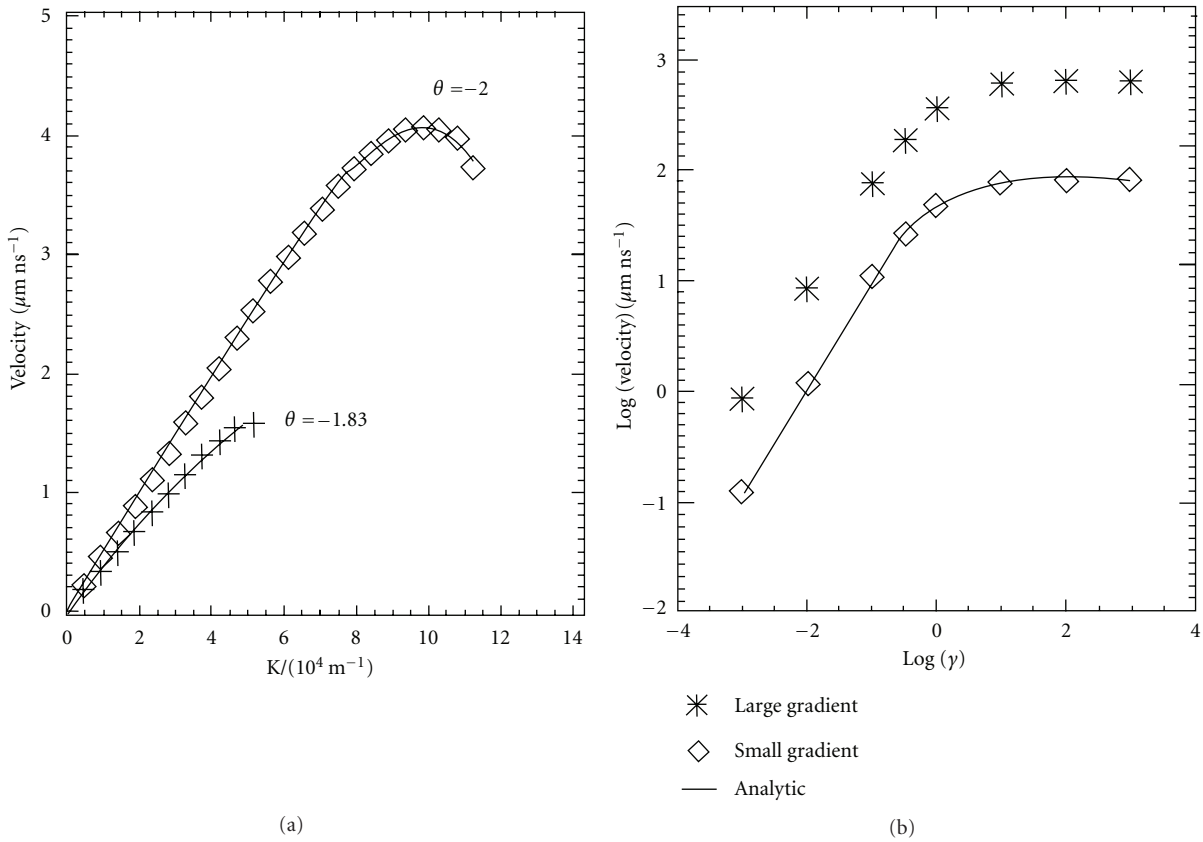

(a) (b)

Figure 12: (a) Drift speed versus phase gradient (wave-vector tilt of holding beam) for a scaled cavity photon to carrier recombination rate $\gamma = 0.01$ (corresponding to a nonradiative carrier lifetime of 1 ns^{-1}) and two-cavity detuning values. The cavity photon lifetime is 10 ps. (b) Log-log plot of CS drift speed versus γ for a fixed scaled detuning ($\theta = -2$) and for two values of the gradient: (stars) $K = 2.38 \times 10^4$ m^{-1}; (diamonds) $K = 1.91 \times 10^5$ m^{-1}. Here, the cavity photon lifetime is 1.5 ps. Figure reproduced from [110].

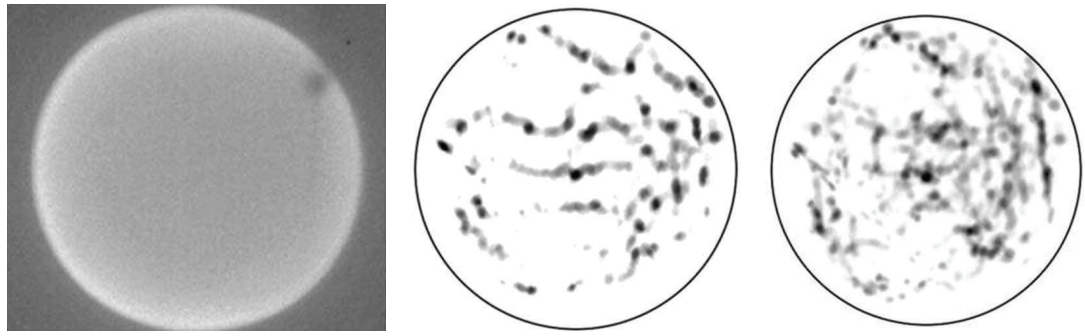

(a) (b) (c)

Figure 13: (a) Spontaneous emission profile of the VCSEL. (b) CSs trajectories when dragged toward the left. (c) Map of the defects in the VCSEL structure as the result of the complete analysis of the CSs trajectories. After [62].

low-intensity regions to repulsive ones. The experimental map is shown in Figure 13 with an inverted contrast. [63] gives a clear proof of the possibility to use the motion properties of localized structures in order to determine the position and strength of defects in semiconductor devices. The spatial resolution is determined by the size of the CS which is in this experiment of the order of $10\,\mu$m. Such a spatial resolution could in principle be increased by working in a different region of parameter space or using devices emitting at shorter wavelength. However, the strength of the proposed method lies in the sensitivity of the CS trajectory to any gradient, should they be smaller than the CS size itself. The practical limitation comes from the preparation of the external gradient and therefore, the quality of the optics that limits the uniformity of the holding beam. Moreover, the method not only allows to detect surface defects, but also can probe bulk defects in the device. This technique has been called soliton force microscopy, since it uses the various potentials felt by CSs in the VCSEL to reveal the map of defects. A similar dragging of CS has also been demonstrated in [54] in a CSL with filtered feedback. In this latter system, an attempt to control the inhomogeneities has also been undertaken in [101] using a Spatial Light Modulator. The idea is to create with an additional, spatially patterned, control beam a gradient that counteracts the effect of the local inhomogeneities by locally varying the refractive index. This results in displaced hysteresis cycles for individual CSs allowing two CSs initially not simultaneously bistable to become controllable in the same parameter regions.

Another interesting aspects of defects in VCSEL devices has been unveiled in [64, 112]. Indeed, defects can under certain circumstances be the source of CSs that may subsequently drift under a gradient, being a controlled gradient or a cavity resonance gradient. This results in the appearance of an almost periodic source of drifting localized states. The average period can be controlled by the phase gradient or by the kind of defect itself. Drifting excitations were also found in a CSL with filtered feedback in [81], while the CS properties remained to be established.

6. Prospects and New Developments

The previous demonstrations of CS using VCSEL devices, either in the optical amplifier or laser regimes, relied on absorptive or gain nonlinearities. CS were observed in the optical field intensity and carrier density components. Several other interesting new directions have been stimulated by these findings, exploring self-localization of different degrees of freedom, using different nonlinearities (see, e.g., [113–115] for theoretical studies of CS in quantum dot materials) or extrapolating the CS concept to three dimensions. In the following, we describe the advances in the fields of polarization CS, cavity soliton polariton and cavity light bullets.

6.1. Polarization CS. Due to the generally circular aperture of VCSELs, polarization of the emission is not constrained into a single direction as in edge-emitting lasers but rather may vary in the whole output plane, depending on the operating conditions (temperature and injection level). This fact has been long recognized and studied in real devices [116–118]. The understanding of the polarization dynamics in VCSELs has been the subject of many theoretical studies and a model [119] now well accepted has emerged, the so-called spin flip model (SFM). Whereas polarization control of VCSELs has represented a major goal of research, polarization switches can also be used in optical communications schemes [120, 121], where stochastic resonance in the polarization dynamics enhances transmission of binary information. The light emitted by a VCSEL is,s in general polarized along one of the two crystallographic directions [110] or $[1\bar{1}0]$ because of crystal anisotropies, and since these anisotropies are weak, it is possible to control the state of emitted polarization. This is also true in broad-area devices [122], while the situation may be more complex for highly divergent modes in even larger devices [123]. In VCSELs with cylindrical symmetry, optical injection [124] or feedback [125, 126] can be employed to control the polarization of light. Since polarized optical injection or optical feedback can both induce bistability [127, 128], all the necessary ingredients are available for CS formation in large-aperture devices. Polarization CS

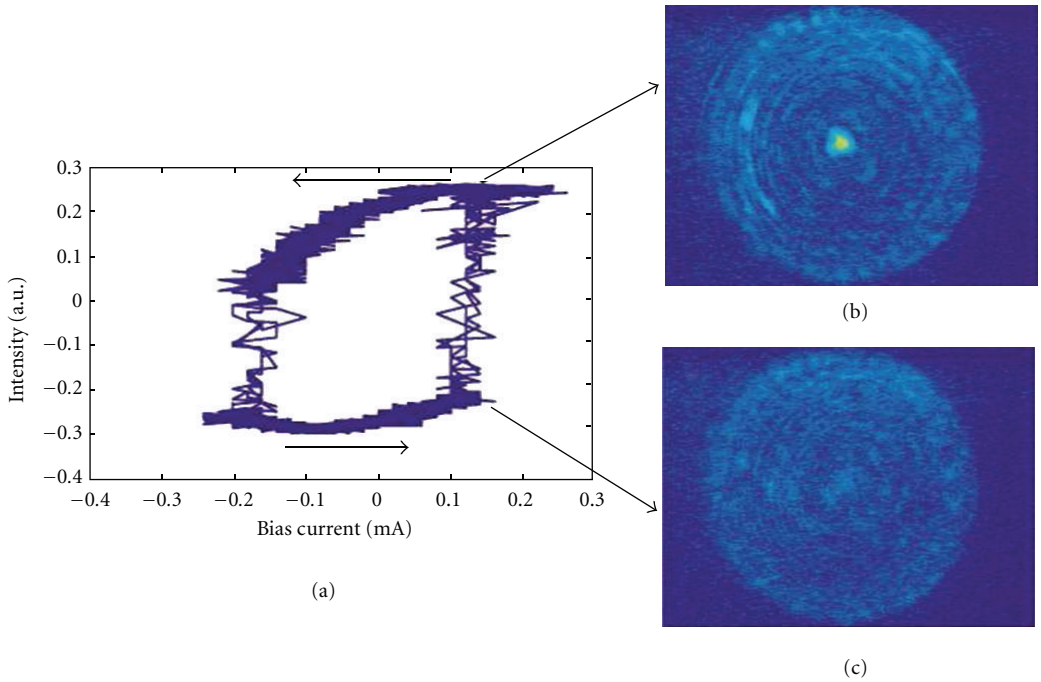

Figure 14: Near-field image of the VCSEL surface when injected by an orthogonally polarized holding beam in the lower (c) and upper (b) branch of the bistability curve (a) obtained by ramping the injected current in the laser. Reprinted with permission from [131]. (© 2011) by the American Physical Society.

could offer the practical advantage of ultrafast switching with low switching energy as was demonstrated in small polarization-bistable devices [129]. Polarization CS were predicted theoretically in [130] in a Kerr cavity with different losses for the two polarization components of the field. They have been experimentally investigated in [131] in a 40 μm diameter VCSEL. The laser, which is shown to emit in a well-defined polarization state just above the laser threshold, is injected by an orthogonally polarized holding beam. A localized state that sits in the center of the device spontaneously switches on and displays a bistable behavior when the injected current is ramped (see Figure 14). These results, though not demonstrating the independence of the localized state from the boundaries principally because of the moderate size of the laser used in the experiment, are encouraging steps towards the demonstration of polarization CS in VCSELs.

6.2. Cavity Light Bullets. Self-localization of light in 3D remains an open challenge [132–136]. The idea of combining the characteristics of a spatial soliton with those of a temporal soliton has been proposed more than 20 years ago [137], and the corresponding object has been termed a light bullet. Light bullets are self-localized states of light in space and time that keep their spatial and temporal profile in the course of propagation: self-focusing can compensate for diffraction and at the same time group velocity dispersion can be compensated by self-phase modulation. Because of the particle-like behavior of optical solitons, 3D self-localized states of light would be intriguing objects possibly leading to new application breakthroughs [138]. Dissipative light bullets are often considered in the context of the complex Ginzburg-Landau equation [139, 140], a model used to describe pulses in mode-locked lasers with a fast saturable absorber. Cavity light bullets share the same properties as dissipative light bullets, in the sense that they are 3D nonlinearly localized states of light. However, CLBs form in a cavity and are thus not freely propagating. CLBs have been proposed and theoretically demonstrated in an extended cavity filled with a saturable absorber medium [141, 142] injected by a holding beam. It was shown that under certain circumstances, spatial filament solitons can destabilize in the propagation direction and form a 3D soliton (cf. Figure 15). These CLBs are addressable and independently controllable as their 2D counterpart. An important feature is that they sit on a non zero background, the stable uniform steady-state. CLBs have also been studied in a similar model including a Kerr focusing nonlinearity, showing that the unstable 3D localized structures then formed can be stabilized via higher-order processes such as multiphoton absorption [143]. A model more suitable for semiconductor systems was studied in [144] with MQWs as the nonlinear material. The model showed that the formation of CLBs requires fast carrier recombination times, since otherwise, the carrier dynamics lags behind the photon dynamics and prevents the formation of a CLB.

CLBs are a theoretical as well as experimental challenge. While the choice of a VCSEL for CS studies in semiconductor systems seems obvious, a variety of semiconductor devices may eventually be used for CLB studies. Among these, bisection edge-emitting lasers are good candidates [145]. Freely propagating light bullets have also been investigated theoretically in nonlinear waveguide arrays, which can be

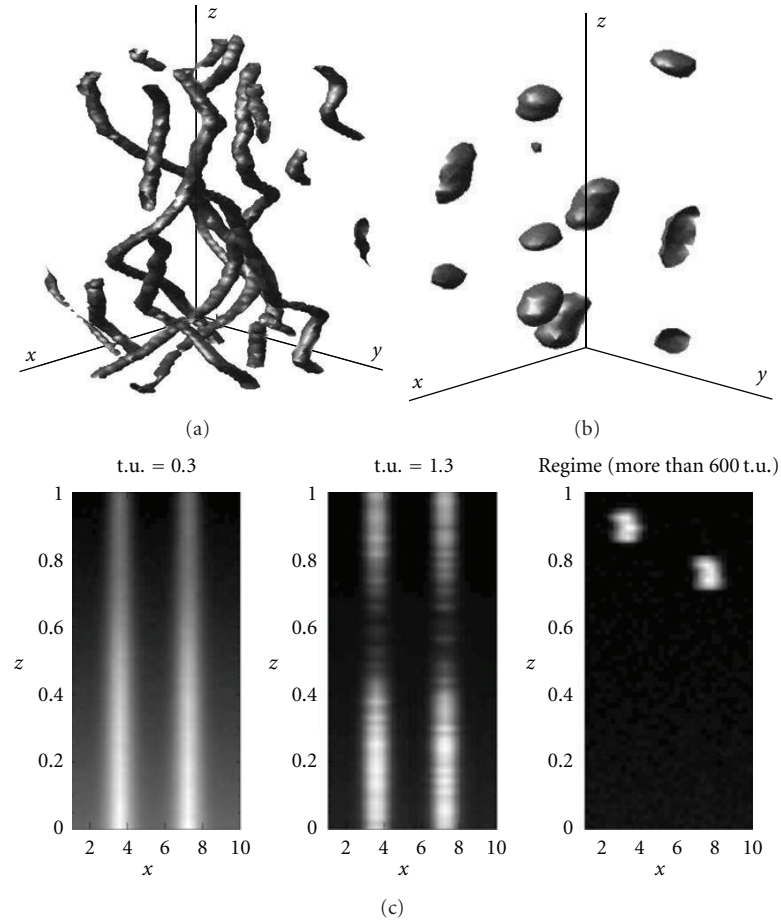

Figure 15: (a, b) Snapshot of 3D filaments and self-confined states in an extended cavity with transverse directions (x, y) and propagation direction z. (c) Three snapshots of a 1D transverse cavity after injection of a writing beam: $t = 0.3$, initial injection; $t = 1.3$, destabilization of the longitudinally uniform solution; $t > 600$, two independent CLBs are formed and propagate in the cavity. Reprinted with permission from [141]. (© 2011) by the American Physical Society.

easily realized in semiconductor materials, in [146–148] and in Bragg gratings [149].

However, the extended cavity configurations used in Section 4 could reveal very interesting regarding CLB demonstration. The idea is to extend the VCSEL cavity to allow for multiple longitudinal modes and temporal mode-locking to take place, while preserving a high Fresnel number ensuring the possibility of multitransverse mode operation [150]. In this configuration, a CLB can be viewed as a mode-locked 2D CS. In [83, 151, 152], using a VCSEL with a frequency selective feedback by a volume Bragg grating in the self-imaging configuration, it was shown that depending on the writing pulse intensity a transient multiple frequency laser CS can be switched on. In most cases the transient oscillations die away after several tens of ns and the final state is a steady, cw laser CS. However, for a high writing pulse intensity an oscillating laser CS can stabilize with a frequency of 3.8 GHz. Because of experimental limitations the modulation depth of the oscillation is not known. Numerical simulations of the system [153] are in fairly good qualitative agreement with the observed behavior and predict the stability of multifrequency laser CSs. The observations can then be interpreted in terms of partially phase-locked external cavity-modes giving rise to quasiperiodically or irregularly pulsing multifrequency laser CSs sitting on a nonzero background.

Self-pulsing localized laser structures are also observed in VCSEL-based schemes with a saturable absorber. In a monolithic vertical cavity laser with saturable absorber [73], self-pulsing localized states are observed. The physical origin of self-pulsing in that case has to be attributed to a Q-switching instability since the cavity has a single-longitudinal mode. The observed behavior is consistent with the experimental observations. In a face to face VCSEL configuration, self-pulsing optical structures have been observed [85] with a pulsing period of 400 ps corresponding to the cavity round-trip time. The physical mechanism for self-pulsing is thus in that case similar to that of the frequency-selective feedback experiment describes earlier. In both cases, the self-pulsing state could not be controlled by an external beam and was not bistable anymore. Control by an external beam of an irregular self-pulsing state has nevertheless been shown in [73].

It has been obtained on a structure composed of several localized spots but the physical mechanism at stake is not clear at the moment. These states are, however, not CLBs, because they develop in microcavities, but they probably constitute a good starting point for further investigation in an extended configuration.

Research on VCSEL-based CLBs is thus concentrated for the moment on extended cavity schemes. While there has been some interesting and encouraging results so far, no conclusive result has been obtained though. One reason lies certainly in the theoretical and numerical difficulty in modeling semiconductor extended cavity systems, since they are nonlinear, multilongitudinal and—transverse mode systems. Moreover, the CLBs obtained this way seem rather different from the original theoretical proposition in [141], and the link to the Ginzburg-Landau type approach to light bullets is not completely clear either. It is anticipated that further studies in the field will help clarify all the physics and the properties of these new self-localized objects and maybe help improve the theoretical comprehension and modeling of semiconductor-based mode-locked lasers [65, 66].

6.3. Cavity Soliton Polariton. Exciton polaritons (also called more simply cavity polaritons or polaritons) are mixed light-matter states arising when an exciton and a cavity-mode are strongly coupled ([154, 155] for a recent review). These states appear when a photon coming from the recombination of an exciton (a bound electron-hole pair) is reabsorbed and reemitted several times before the photon escapes from the microcavity. The cavity-exciton coupling gives rise to two resonances separated by the so-called Rabi splitting observed in the reflectivity spectrum of the microcavity, through a mechanism analogous to the anticrossing in the eigenenergies of a system composed of two coupled oscillators. This normal-mode coupling [156] is characterized by the dispersion curve depicted, for example, in Figure 1(a) in [157]. Exciton polaritons are fascinating quantum objects with bosonic properties in which Bose-Einstein condensation was recently observed [158] at temperatures much higher than in atomic clouds (and even at room temperature in [159]). An important feature in the context of CS is the giant χ^3-type nonlinearity exhibited by exciton polaritons due to the coherent polariton-polariton scattering: two pump polaritons with in-plane wave vector k_p can scatter in one polariton with in-plane wave vector $2k_p$ and one with 0 in-plane wave-vector. This coherent process must fulfill phase matching and energy conservation conditions, and can be obtained in two different ways. The first one, in the degenerate case, with normal incidence pump beam which gives rise to an optical nonlinearity analogous to a Kerr nonlinearity, with the difference that the index of refraction no longer depends on the input beam intensity but rather on the polariton density. The second one in the nondegenerate case in a parametric amplification configuration, at the so-called "magic-angle" (inflection point in the lower-polariton dispersion curve) with nonzero pump wave vector [160]. Bistability has been observed in both the degenerate [161] and the nondegenerate case [162]. Another mechanism is also predicted to lead to bistability in the strong coupling regime using the nonlinear bleaching of the Rabi-splitting [163] under high pumping excitation. However, there has been no convincing experimental observations of such a mechanism so far. A few experimental observations are associated with the simultaneous presence of the weak and strong coupling signatures in the spectrum, and bistability is associated to the bare cavity mode [164, 165]. Bistability has also been observed in a polariton diode [166], where the intracavity electric field is responsible for the strong to weak coupling abrupt switching.

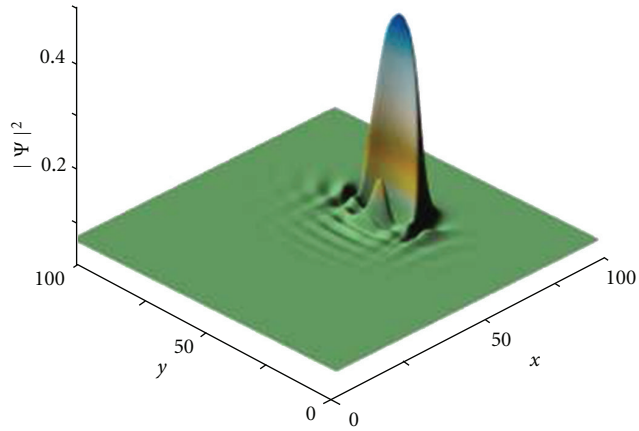

Figure 16: 2D self-localized bright CS polariton as predicted in [170]. Reprinted with permission from [170]. (© 2011) by the American Physical Society.

Bistability being again one key ingredient for CS formation, several authors have studied how nonlinear and spatial effects (diffraction in particular) can mix to allow self-localized states appearance. Indications of self-localization were reported in [167], where local bistability, as well as localized bright and dark optical structures are reported in a microcavity with several QWs as active medium, brought to low temperature (4 K). However, a clear demonstration of polariton CS is missing, since no demonstration of independent excitation has been reported. All these results stimulated theoretical work on polariton CS. In addition to the large optical nonlinearity exhibited in this system, which is interesting because it allows the realization of low pump-power nonlinear optical devices [168], exciton polariton-based systems are expected to display very fast switching times too [169], a few orders of magnitude smaller than in the weak-coupling regime. Moreover, the quantum nature of exciton polaritons could open new prospects in the field of CS applied to information processing or parallel computation though practical schemes are not very clear at the moment (Figure 16).

Dark polariton solitons were first predicted to appear [171] in a cavity sustaining exciton polaritons, when the lower polariton branch is excited at normal incidence. The fact that bright CS polaritons were found to be unstable in that case is related to the defocusing nature of the exciton-polariton nonlinearity. Using the dispersion properties of the lower polariton branch near its inflection point ($|k| \simeq 1$ in Figure 1(a)) in [157]), it was later shown [172] that 1D bright

CS polaritons could be obtained. The stabilization of these states rely on the existence of higher-order spatial dispersion terms that can counteract the repulsive nonlinearity. These CS polaritons are moving objects, since the first order dispersion is nonzero at the inflection point. In 2D, use of a confining potential in the perpendicular direction to the inclined pump beam has been proposed to obtain 2D localized states. The authors claim that their theoretical predictions are in good agreement with the almost simultaneous experimental observation reported in [157] of moving "quasilocalized" polaritons. The latter authors have however a different interpretation in terms of the straightening of the Bogolyubov dispersion in superfluids.

In spite of the opposite signs of dispersion in polaritons excited close to the magic angle, truly 2D self-confined polaritons have nevertheless been obtained numerically in a recent work [170]. Starting from the 1D bright CS polariton conditions demonstrated in [172], the authors show that there exists a range of excitation intensities for which the width of the localized state remains constant in both directions. While in the propagation direction the explanation for self-localization remains the same as in the 1D case, in the perpendicular direction self-localization is attributed to the parametric nonlinearity: the 2D CS polariton is thus stable in both directions thanks to different physical mechanisms, each of them sustaining their family of 1D self-localized states.

Other theoretical studies have focused on different physical mechanism for CS polariton formation. In [173], taking into account the polarization degree of freedom of exciton polaritons, the authors show 1D vectorial bright and dark CS polaritons formation. Exploring in [174] the saturation of exciton-photon coupling, the author shows that normal incidence, resting CS polaritons may exist. However, stability conditions impose then unrealistically large exciton dispersions (or very small exciton effective mass).

In conclusion, even though the experimental observations in [157] are encouraging, CS polaritons observation and control remain an open challenge and may open new prospects in the field because of the different physics involved. In terms of possible applications, in spite of the quantitative improvements in the switching speed and holding beam power needed for their formation, the question remains whether the quantum nature of the exciton-polariton may be used for still unexplored functionalities.

Acknowledgments

The authors wish to thank A. Amo and J. Bloch for useful discussions and comments on the paper.

References

[1] L. Lugiato, F. Prati, G. Tissoni et al., "Cavity solitons in semiconductor devices," in *Dissipative Solitons: From Optics to Biology and Medicine*, vol. 751 of *Lecture Notesin Physics*, pp. 1–42, Springer, Berlin Heidelberg, Germany, 2008.

[2] G. Tissoni, K. M. Aghdami, F. Prati, M. Brambilla, and L. A. Lugiato, " Cavity soliton laser based on a VCSEL with saturable absorber," in *Localized States in Physics: Solitons and Patterns*, O. Descalzi, M. Clerc, S. Residori, and G. Assanto, Eds., pp. 187–211, Springer, Berlin Heidelberg, Germany, 2011.

[3] T. Ackemann, W. J. Firth, and G. L. Oppo, "Fundamentalsand applications of spatial dissipative solitons in photonic devices," in *Advances in Atomic Molecular and Optical Physics*, P. R. B. E. Arimondo and C. C. Lin, Eds., vol. 57 of *AdvancesIn Atomic, Molecular, and Optical Physics*, chapter 6, pp. 323–421, Academic Press, 2009.

[4] R. Kuszelewicza, S. Barbay, G. Tissoni, and G. Almuneau, "Editorial on dissipative optical solitons," *European Physical Journal D*, vol. 59, no. 1, pp. 1–2, 2010.

[5] H. G. Solari, M. Natiello, and G. Mindlin, *Nonlinear Dynamics: A Two-Way Trip from Physics to Math*, IOP Publishers, London, UK, 1996.

[6] R. Gilmore and M. Lefranc, *The Topology of Chaos, Alice in Stretch and Squeeze land*, Wiley, New York, NY, USA, 2002.

[7] F. Moss, L. A. Lugiato, and W. Schleigh, Eds., *Noise and Chaos in Nonlinear Dynamical Systems*, Cambridge University Press, New York, NY, USA, 1990.

[8] B. Belousov, "A periodic reaction and its mechanism," in *Oscillationsand Traveling Waves in Chemical Systems*, R. Field and M. Burger, Eds., pp. 605–613, Wiley, New York, NY, USA, 1985.

[9] J. C. Roux, R. H. Simoyi, and H. L. Swinney, "Observation of a strange attractor," *Physica D*, vol. 8, no. 1-2, pp. 257–266, 1983.

[10] F. T. Arecchi, R. Meucci, G. Puccioni, and J. Tredicce, "Experimental evidence of subharmonic bifurcations, multistability, and turbulence in a Q-switched gas laser," *Physical Review Letters*, vol. 49, no. 17, pp. 1217–1220, 1982.

[11] N. B. Abraham, P. Mandel, and L. M. Narducci, "I dynamical instabilities and pulsations in lasers," *Progress in Optics*, vol. 25, pp. 1–190, 1988.

[12] F. T. Arecchi, G. L. Lippi, G. P. Puccioni, and J. R. Tredicce, "Deterministic chaos in laser with injected signal," *Optics Communications*, vol. 51, no. 5, pp. 308–314, 1984.

[13] J. R. Tredicce, F. T. Arecchi, G. L. Lippi, and G. P. Puccioni, "Instabilities in lasers with an injected signal," *Journal of the Optical Society of America B*, vol. 2, no. 1, pp. 173–183, 1985.

[14] L. A. Lugiato, L. M. Narducci, D. K. Bandy, and C. A. Pennise, "Breathing, spiking and chaos in a laser with injected signal," *Optics Communications*, vol. 46, no. 1, pp. 64–68, 1983.

[15] L. M. Narducci, J. R. Tredicce, L. A. Lugiato, N. B. Abraham, and D. K. Bandy, "Multimode laser with an injected signal: steady-state and linear stability analysis," *Physical Review A*, vol. 32, no. 3, pp. 1588–1595, 1985.

[16] H. G. Solari and G. L. Oppo, "Laser with injected signal: perturbation of an invariant circle," *Optics Communications*, vol. 111, no. 1-2, pp. 173–190, 1994.

[17] F. A. N. B. Abraham and l. Lugiato, Eds., *Instabilities and Chaos in Quantum Optics*, vol. 2, Plenum Press, New York, 1988.

[18] S. Wieczorek, B. Krauskopf, and D. Lenstra, "Unifying view of bifurcations in a semiconductor laser subject to optical injection," *Optics Communications*, vol. 172, no. 1, pp. 279–295, 1999.

[19] G. Vaschenko, M. Giudici, J. J. Rocca, C. S. Menoni, J. R. Tredicce, and S. Balle, "Temporal dynamics of semiconductor lasers with optical feedback," *Physical Review Letters*, vol. 81, no. 25, pp. 5536–5539, 1998.

[20] B. Krauskopf and D. Lenstra, Eds., *Fundamental Issues of Nonlinear Laser Dynamics*, AIP, New York, NY, USA, 2000.

[21] P. Coullet, L. Gil, and F. Rocca, "Optical vortices," *Optics Communications*, vol. 73, no. 5, pp. 403–408, 1989.

[22] J. R. Tredicce, E. J. Quel, A. M. Ghazzawi et al., "Spatial and temporal instabilities in a CO2 laser," *Physical Review Letters*, vol. 62, no. 11, pp. 1274–1277, 1989.

[23] P. L. Ramazza, S. Ducci, S. Boccaletti, and F. T. Arecchi, "Localized versus delocalized patterns in a nonlinear optical interferometer," *Journal of Optics B*, vol. 2, no. 3, pp. 399–405, 2000.

[24] R. Holzner, P. Eschle, A. W. McCord, and D. M. Warrington, "Transverse "bouncing" of polarized laser beams in sodium vapor," *Physical Review Letters*, vol. 69, no. 15, pp. 2192–2195, 1992.

[25] M. Brambilla, L. A. Lugiato, V. Penna, F. Prati, C. Tamm, and C. O. Weiss, "Transverse laser patterns. II. Variational principle for pattern selection, spatial multistability, and laser hydrodynamics," *Physical Review A*, vol. 43, no. 9, pp. 5114–5120, 1991.

[26] C. Green, G. B. Mindlin, E. J. D'Angelo, H. G. Solari, and J. R. Tredicce, "Spontaneous symmetry breaking in a laser: the experimental side," *Physical Review Letters*, vol. 65, no. 25, pp. 3124–3127, 1990.

[27] R. L. Ruiz, G. B. Mindlin, C. Pérez García, and J. Tredicce, "Mode-mode interaction for a CO2 laser with imperfect O(2) symmetry," *Physical Review A*, vol. 47, no. 1, pp. 500–509, 1993.

[28] A. B. Coates, C. O. Weiss, C. Green et al., "Dynamical transverse laser patterns. II. Experiments," *Physical Review A*, vol. 49, no. 2, pp. 1452–1466, 1994.

[29] G. Huyet, M. C. Martinoni, J. R. Tredicce, and S. Rica, "Spatiotemporal dynamics of lasers with a large fresnel number," *Physical Review Letters*, vol. 75, no. 22, pp. 4027–4030, 1995.

[30] M. Brambilla, L. A. Lugiato, F. Prati, L. Spinelli, and W. J. Firth, "Spatial soliton pixels in semiconductor devices," *Physical Review Letters*, vol. 79, no. 11, pp. 2042–2045, 1997.

[31] D. Michaelis, U. Peschel, and F. Lederer, "Multistable localized structures and superlattices in semiconductor optical resonators," *Physical Review A*, vol. 56, no. 5, pp. R3366–R3369, 1997.

[32] G. Tissoni, L. Spinelli, M. Brambilla, T. Maggipinto, I. M. Perrini, and L. A. Lugiato, "Cavity solitons in passive bulk semiconductor microcavities. I. Microscopic model and modulational instabilities," *Journal of the Optical Society of America B*, vol. 16, no. 11, pp. 2083–2094, 1999.

[33] R. Kuszelewicz, I. Ganne, I. Sagnes, G. Slekys, and M. Brambilla, "Optical self-organization in bulk and multiquantum well GaAIAs microresonators," *Physical Review Letters*, vol. 84, no. 26, pp. 6006–6009, 2000.

[34] V. B. Taranenko, I. Ganne, R. J. Kuszelewicz, and C. O. Weiss, "Patterns and localized structures in bistable semiconductor resonators," *Physical Review A*, vol. 61, no. 6, pp. 063818–063811, 2000.

[35] T. Ackemann, S. Barland, M. Cara et al., "Spatial mode structure of bottom-emitting broad-area vertical-cavity surface-emitting lasers," *Journal of Optics B*, vol. 2, no. 3, pp. 406–412, 2000.

[36] T. Ackemann, S. Barland, J. R. Tredicce et al., "Spatial structure of broad-area vertical-cavity regenerative amplifiers," *Optics Letters*, vol. 25, no. 11, pp. 814–816, 2000.

[37] N. N. Rosanov and G. V. Khodova, "Autosolitons in bistable interferometers," *Optics and Spectroscopy*, vol. 65, pp. 449–450, 1988.

[38] G. S. McDonald and W. J. Firth, "Spatial solitary-wave optical memory," *Journal of the Optical Society of America B*, vol. 7, pp. 1328–1335, 1990.

[39] M. Tlidi, P. Mandel, and R. Lefever, "Localized structures and localized patterns in optical bistability," *Physical Review Letters*, vol. 73, no. 5, pp. 640–643, 1994.

[40] W. J. Firth and A. J. Scroggie, "Optical bullet holes: robust controllable localized states of a nonlinear cavity," *Physical Review Letters*, vol. 76, no. 10, pp. 1623–1626, 1996.

[41] L. Spinelli, G. Tissoni, M. Tarenghi, and M. Brambilla, "First principle theory for cavity solitons in semiconductor microresonators," *European Physical Journal D*, vol. 15, no. 2, pp. 257–266, 2001.

[42] G. I. A. Stegeman, D. N. Christodoulides, and M. Segev, "Optical spatial solitons: historical perspectives," *IEEE Journal on Selected Topics in Quantum Electronics*, vol. 6, no. 6, pp. 1419–1427, 2000.

[43] P. Coullet, C. Riera, and C. Tresser, "Stable static localized structures in one dimension," *Physical Review Letters*, vol. 84, no. 14, pp. 3069–3072, 2000.

[44] W. J. Firth, L. Columbo, and A. J. Scroggie, "Proposed resolution of theory-experiment discrepancy in homoclinic snaking," *Physical Review Letters*, vol. 99, no. 10, Article ID 104503, 2007.

[45] S. Barbay, X. Hachair, T. Elsass, I. Sagnes, and R. Kuszelewicz, "Homoclinic snaking in a semiconductor-based optical system," *Physical Review Letters*, vol. 101, no. 25, Article ID 253902, 2008.

[46] B. Schäpers, M. Feldmann, T. Ackemann, and W. Lange, "Interaction of localized structures in an optical pattern-forming system," *Physical Review Letters*, vol. 85, no. 4, pp. 748–751, 2000.

[47] N. N. Rosanov and G. V. Khodova, "Diffractive autosolitons in nonlinear interferometers," *Journal of the Optical Society of America B*, vol. 7, pp. 1057–1065, 1990.

[48] M. Saffman, D. Montgomery, and D. Z. Anderson, "Collapse of a transverse-mode continuum in a self-imaging photorefractively pumped ring resonator," *Optics Letters*, vol. 19, no. 8, pp. 518–520, 1994.

[49] R. Neubecker, G. L. Oppo, B. Thuering, and T. Tschudi, "Pattern formation in a liquid-crystal light valve with feedback, including polarization, saturation, and internal threshold effects," *Physical Review A*, vol. 52, no. 1, pp. 791–808, 1995.

[50] S. Barland, J. R. Tredicce, M. Brambilla et al., "Cavity solitons work as pixels in semiconductors," *Nature*, vol. 419, no. 6908, pp. 699–702, 2002.

[51] M. Grabherr, R. Jäger, M. Miller et al., "Bottom-emitting VCSEL's for high-CW optical output power," *IEEE Photonics Technology Letters*, vol. 10, no. 8, pp. 1061–1063, 1998.

[52] M. Grabherr, M. Miller, R. Jäger et al., "High-power VCSEL's: single devices and densely packed 2-D-arrays," *IEEE Journal on Selected Topics in Quantum Electronics*, vol. 5, no. 3, pp. 495–502, 1999.

[53] M. Miller, M. Grabherr, R. King, R. Jäger, R. Michalzik, and K. J. Ebeling, "Improved output performance of high-power VCSELs," *IEEE Journal on Selected Topics in Quantum Electronics*, vol. 7, no. 2, pp. 210–216, 2001.

[54] Y. Tanguy, T. Ackemann, W. J. Firth, and R. Jäger, "Realization of a semiconductor-based cavity soliton laser," *Physical Review Letters*, vol. 100, no. 1, Article ID 013907, 2008.

[55] P. Genevet, S. Barland, M. Giudici, and J. R. Tredicce, "Cavity soliton laser based on mutually coupled semiconductor microresonators," *Physical Review Letters*, vol. 101, no. 12, Article ID 123905, 2008.

[56] S. Fedorov, D. Michaelis, U. Peschel et al., "Effects of spatial inhomogeneities on the dynamics of cavity solitons in

quadratically nonlinear media," *Physical Review E*, vol. 64, no. 3, Article ID 036610, pp. 366101–366108, 2001.

[57] A. J. Scroggie, J. Jeffers, G. McCartney, and G. L. Oppo, "Reversible soliton motion," *Physical Review E*, vol. 71, no. 4, Article ID 046602, pp. 046602/1–046602/5, 2005.

[58] X. Hachair, S. Barland, L. Furfaro et al., "Cavity solitons in broad-area vertical-cavity surface-emitting lasers below threshold," *Physical Review A*, vol. 69, no. 4, article 043817, 2004.

[59] X. Hachair, F. Pedaci, E. Caboche et al., "Cavity solitons in a driven VCSEL above threshold," *IEEE Journal on Selected Topics in Quantum Electronics*, vol. 12, no. 3, pp. 339–351, 2006.

[60] R. Michalzik, M. Grabherr, and K. J. Ebeling, "High-power vcsels: modelingand experimental characterization," in *Proceedings of the SPIE 3286 (SPIE '98)*, K. D. Choquette and R. A. Morgan, Eds., vol. 3286, pp. 206–219, 1998.

[61] T. Camps, V. Bardinal, E. Havard et al., "Management of the electrical injection uniformity in broad-area top-emitting VCSELs," *European Physical Journal D*, vol. 59, no. 1, pp. 53–57, 2010.

[62] M. Dabbicco, T. Maggipinto, and M. Brambilla, "Optical bistability and stationary patterns in photonic-crystal vertical-cavity surface-emitting lasers," *Applied Physics Letters*, vol. 86, no. 2, Article ID 021116, 2005.

[63] F. Pedaci, G. Tissoni, S. Barland, M. Giudici, and J. Tredicce, "Mapping local defects of extended media using localized structures," *Applied Physics Letters*, vol. 93, no. 11, Article ID 111104, 2008.

[64] E. Caboche, F. Pedaci, P. Genevet et al., "Microresonator defects as sources of drifting cavity solitons," *Physical Review Letters*, vol. 102, no. 16, Article ID 163901, 2009.

[65] U. Keller, "Recent developments in compact ultrafast lasers," *Nature*, vol. 424, no. 6950, pp. 831–838, 2003.

[66] U. Keller and A. C. Tropper, "Passively modelocked surface-emitting semiconductor lasers," *Physics Reports*, vol. 429, no. 2, pp. 67–120, 2006.

[67] S. Barbay, Y. Ménesguen, I. Sagnes, and R. Kuszelewicz, "Cavity optimization of optically pumped broad-area microcavity lasers," *Applied Physics Letters*, vol. 86, no. 15, Article ID 151119, pp. 1–3, 2005.

[68] S. Barbay, Y. Ménesguen, X. Hachair, L. Leroy, I. Sagnes, and R. Kuszelewicz, "Incoherent and coherent writing and erasure of cavity solitons in an optically pumped semiconductor amplifier," *Optics Letters*, vol. 31, no. 10, pp. 1504–1506, 2006.

[69] D. G. H. Nugent, R. G. S. Plumb, M. A. Fisher, and D. A. O. Davies, "Self-pulsations in vertical-cavity surface-emitting lasers," *Electronics Letters*, vol. 31, no. 1, pp. 43–44, 1995.

[70] S. F. Lim, J. A. Hudgings, G. S. Li, W. Yuen, K. Y. Lau, and C. J. Chang-Hasnain, "Self-pulsating and bistable VCSEL with controllable intracavity quantum-well saturable absorber," *Electronics Letters*, vol. 33, no. 20, pp. 1708–1710, 1997.

[71] K. D. Choquette, H. Q. Hou, K. L. Lear et al., "Self-pulsing oxide-confined vertical-cavity lasers with ultralow operating current," *Electronics Letters*, vol. 32, no. 5, pp. 459–460, 1996.

[72] A. J. Fischer, W. W. Chow, K. D. Choquette, A. A. Allerman, and K. M. Geib, "Q-switched operation of a coupled-resonator vertical-cavity laser diode," *Applied Physics Letters*, vol. 76, no. 15, pp. 1975–1977, 2000.

[73] T. Elsass, K. Gauthron, G. Beaudoin, I. Sagnes, R. Kuszelewicz, and S. Barbay, "Control of cavity solitons and dynamical states in a monolithic vertical cavity laser with saturable absorber," *European Physical Journal D*, vol. 59, no. 1, pp. 91–96, 2010.

[74] U. Bortolozzo, S. Residori, and P. L. Ramazza, "Optical structures and their control in a liquid-crystal-light-valve experiment," *Molecular Crystals and Liquid Crystals*, vol. 450, no. 1, pp. 141–162, 2006.

[75] T. Elsass, K. Gauthron, G. Beaudoin, I. Sagnes, R. Kuszelewicz, and S. Barbay, "Fast manipulation of laser localized structures in a monolithic vertical cavity with saturable absorber," *Applied Physics B*, vol. 98, no. 2-3, pp. 327–331, 2010.

[76] X. Hachair, L. Furfaro, J. Javaloyes et al., "Cavity-solitons switching in semiconductor microcavities," *Physical Review A*, vol. 72, no. 1, Article ID 013815, 2005.

[77] S. Barbay and R. Kuszelewicz, "Physical model for the incoherent writing/erasure of cavity solitons in semiconductor optical amplifiers," *Optics Express*, vol. 15, no. 19, pp. 12457–12463, 2007.

[78] L. Columbo, L. Gil, and J. Tredicce, "Could cavity solitons exist in bidirectional ring lasers?" *Optics Letters*, vol. 33, no. 9, pp. 995–997, 2008.

[79] R. Vilaseca, M. C. Torrent, J. García-Ojalvo, M. Brambilla, and M. S. Miguel, "Two-photon cavity solitons in active optical media," *Physical Review Letters*, vol. 87, no. 8, Article ID 083902, pp. 839021–839024, 2001.

[80] V. Ahufinger, J. García-Ojalvo, J. Mompart, M. C. Torrent, R. Corbalán, and R. Vilaseca, "Cavity solitons in two-level lasers with dense amplifying medium," *Physical Review Letters*, vol. 91, no. 8, pp. 839011–839014, 2003.

[81] Y. Tanguy, N. Radwell, T. Ackemann, and R. Jäger, "Characteristics of cavity solitons and drifting excitations in broad-area vertical-cavity surface-emitting lasers with frequency-selective feedback," *Physical Review A*, vol. 78, no. 2, Article ID 023810, 2008.

[82] P. V. Paulau, D. Gomila, T. Ackemann, N. A. Loiko, and W. J. Firth, "Self-localized structures in vertical-cavity surface-emitting lasers with external feedback," *Physical Review E*, vol. 78, no. 1, Article ID 016212, 2008.

[83] N. Radwell, C. McIntyre, A. J. Scroggie, G. L. Oppo, W. J. Firth, and T. Ackemann, "Switching spatial dissipative solitons in a VCSEL with frequency selective feedback," *European Physical Journal D*, vol. 59, no. 1, pp. 121–131, 2010.

[84] N. Radwell and T. Ackemann, "Characteristics of laser cavity solitons in a vertical-cavity surface-emitting laser with feedback from a volume Bragg grating," *IEEE Journal of Quantum Electronics*, vol. 45, no. 11, pp. 1388–1395, 2009.

[85] P. Genevet, S. Barland, M. Giudici, and J. R. Tredicce, "Stationary localized structures and pulsing structures in a cavity soliton laser," *Physical Review A*, vol. 79, no. 3, Article ID 033819, 2009.

[86] P. Genevet, L. Columbo, S. Barland, M. Giudici, L. Gil, and J. R. Tredicce, "Multistable monochromatic laser solitons," *Physical Review A*, vol. 81, no. 5, Article ID 053839, 2010.

[87] L. Columbo, L. Gila, and P. Genevet, "Theoretical description of the transverse localised structures in a face to face VCSEL configuration," *European Physical Journal D*, vol. 59, no. 1, pp. 97–107, 2010.

[88] P. Genevet, S. Barland, M. Giudici, and J. R. Tredicce, "Bistable and addressable localized vortices in semiconductor lasers," *Physical Review Letters*, vol. 104, no. 22, Article ID 223902, 2010.

[89] N. N. Rozanov, S. V. Fedorov, and A. N. Shatsev, "Nonstationary multivortex and fissionable soliton-like structures of laser radiation," *Optics and Spectroscopy*, vol. 95, no. 6, pp. 843–848, 2003.

[90] S. V. Fedorov and N. N. Rosanov, "Diffraction switching waves and autosolitonsin a laser with saturable absorption," *Optics and Spectroscopy*, vol. 72, no. 6, pp. 782–785, 1992.

[91] A. G. Vladimirov, S. V. Fedorov, N. A. Kaliteevskii, G. V. Khodova, and N. N. Rosanov, "Numerical investigation of laser localized structures," *Journal of Optics B*, vol. 1, no. 6, pp. 101–106, 1999.

[92] M. Bache, F. Prati, G. Tissoni et al., "Cavity soliton laser based on VCSEL with saturable absorber," *Applied Physics B*, vol. 81, no. 7, pp. 913–920, 2005.

[93] S. V. Fedorov, N. N. Rozanov, and A. N. Shatsev, "Two-dimensional solitons in B-class lasers with saturable absorption," *Optics and Spectroscopy*, vol. 102, no. 3, pp. 449–455, 2007.

[94] F. Prati, P. Caccia, G. Tissoni, L. A. Lugiato, K. M. Aghdami, and H. Tajalli, "Effects of carrier radiative recombination on a VCSEL-based cavity soliton laser," *Applied Physics B*, vol. 88, no. 3, pp. 405–410, 2007.

[95] K. M. Aghdami, F. Prati, P. Caccia et al., "Comparison of different switching techniques in a cavity soliton laser," *European Physical Journal D*, vol. 47, no. 3, pp. 447–455, 2008.

[96] N. N. Rosanov, S. V. Fedorov, and A. N. Shatsev, "Two-dimensional laser soliton complexes with weak, strong, and mixed coupling," *Applied Physics B*, vol. 81, no. 7, pp. 937–943, 2005.

[97] N. N. Rosanov, S. V. Fedorov, and A. N. Shatsev, "Curvilinear motion of multivortex laser-soliton complexes with strong and weak coupling," *Physical Review Letters*, vol. 95, no. 5, Article ID 053903, pp. 1–4, 2005.

[98] P. Genevet, M. Turconi, S. Barland, M. Giudici, and J. R. Tredicce, "Mutual coherence of laser solitons in coupled semiconductor resonators," *European Physical Journal D*, vol. 59, no. 1, pp. 109–114, 2010.

[99] S. V. Fedorov, A. G. Vladimirov, G. V. Khodova, and N. N. Rosanov, "Effect of frequency detunings and finite relaxation rates on laser localized structures," *Physical Review E*, vol. 61, no. 5, pp. 5814–5824, 2000.

[100] F. Prati, G. Tissoni, L. A. Lugiato, K. M. Aghdami, and M. Brambilla, "Spontaneously moving solitons in a cavity soliton laser with circular section," *European Physical Journal D*, vol. 59, no. 1, pp. 73–79, 2010.

[101] N. Radwell, P. Rose, C. Cleff, C. Denz, and T. Ackemann, "Compensation of spatial inhomogeneities in a cavity soliton laser using a spatial light modulator," *Optics Express*, vol. 18, no. 22, pp. 23121–23132, 2010.

[102] N. N. Rosanov, "Switching waves, autosolitons, and parallel digital-analogous optical computing," in *Transverse Patterns in Nonlinear Optics*, N. N. Rosanov, Ed., vol. 1840, pp. 130–143, 1992.

[103] F. Pedaci, P. Genevet, S. Barland, M. Giudici, and J. R. Tredicce, "Positioning cavity solitons with a phase mask," *Applied Physics Letters*, vol. 89, no. 22, Article ID 221111, 2006.

[104] L. V. Hau, S. E. Harris, Z. Dutton, and C. H. Behroozi, "Light speed reduction to 17 metres per second in an ultracold atomic gas," *Nature*, vol. 397, no. 6720, pp. 594–598, 1999.

[105] Y. Okawachi, M. S. Bigelow, J. E. Sharping et al., "Tunable all-optical delays via brillouin slow light in an optical fiber," *Physical Review Letters*, vol. 94, no. 15, article 153902, 2005.

[106] J. E. Sharping, Y. Okawachi, and A. L. Gaeta, "Wide bandwidth slow light using a Raman fiber amplifier," *Optics Express*, vol. 13, no. 16, pp. 6092–6098, 2005.

[107] M. van der Poel, J. Mørk, and J. M. Hvam, "Controllable delay of ultrashort pulses in a quantum dot optical amplifier," *Optics Express*, vol. 13, no. 20, pp. 8032–8037, 2005.

[108] J. T. Mok, C. M. de Sterke, I. C. M. Littler, and B. J. Eggleton, "Dispersionless slow light using gap solitons," *Nature Physics*, vol. 2, no. 11, pp. 775–780, 2006.

[109] B. Schäpers, T. Ackemann, and W. Lange, "Characteristics and possible applications of localized structures in an optical pattern-forming system," in *Proceedings of the 2nd Nonlinear Optical Beam and Pulse Propagation (SPIE '01)*, vol. 4271, pp. 130–137, 2001.

[110] F. Pedaci, S. Barland, E. Caboche et al., "All-optical delay line using semiconductor cavity solitons," *Applied Physics Letters*, vol. 92, no. 1, article 011101, 2008.

[111] G. Kozyreff, P. Assemat, and S. J. Chapman, "Influence of boundaries on localized patterns," *Physical Review Letters*, vol. 103, no. 16, article 164501, 2009.

[112] E. Caboche, S. Barland, M. Giudici, J. Tredicce, G. Tissoni, and L. A. Lugiato, "Cavity-soliton motion in the presence of device defects," *Physical Review A*, vol. 80, no. 5, Article ID 053814, 2009.

[113] S. Barbay, J. Koehler, R. Kuszelewicz, T. Maggipinto, I. M. Perrini, and M. Brambilla, "Optical patterns and cavity solitons in quantum-dot microresonators," *IEEE Journal of Quantum Electronics*, vol. 39, no. 2, pp. 245–254, 2003.

[114] I. M. Perrini, S. Barbay, T. Maggipinto, M. Brambilla, and R. Kuszelewicz, "Model for optical pattern and cavity soliton formation in a microresonator with self-assembled semiconductor quantum dots," *Applied Physics B*, vol. 81, no. 7, pp. 905–912, 2005.

[115] M. Brambilla, T. Maggipinto, I. M. Perrini, S. Barbay, and R. Kuszelewicz, "Modeling pattern formation and cavity solitons in quantum dot optical microresonators in absorbing and amplifying regimes," *Chaos*, vol. 17, no. 3, article 037119, 2007.

[116] K. D. Choquette, D. A. Richie, and R. E. Leibenguth, "Temperature dependence of gain-guided vertical-cavity surface emitting laser polarization," *Applied Physics Letters*, vol. 64, no. 16, pp. 2062–2064, 1994.

[117] C. J. Chang-Hasnain, J. P. Harbison, L. T. Florez, and N. G. Stoffel, "Polarisation characteristics of quantum well vertical cavity surface emitting lasers," *Electronics Letters*, vol. 27, no. 2, pp. 163–165, 1991.

[118] C. J. Chang-Hasnain, J. P. Harbison, G. Hasnain, A. C. von Lehmen, L. T. Florez, and N. G. Stoffel, "Dynamic, polarization, and transverse mode characteristics of vertical cavity surface emitting lasers," *IEEE Journal of Quantum Electronics*, vol. 27, no. 6, pp. 1402–1409, 1991.

[119] M. S. Miguel, Q. Feng, and J. V. Moloney, "Light-polarization dynamics in surface-emitting semiconductor lasers," *Physical Review A*, vol. 52, no. 2, pp. 1728–1739, 1995.

[120] S. Barbay, G. Giacomelli, and F. Marin, "Noise-assisted transmission of binary information: theory and experiment," *Physical Review E*, vol. 63, no. 5, pp. 511101–511109, 2001.

[121] S. Barbay, G. Giacomelli, and F. Marin, "Experimental evidence of binary aperiodic stochastic resonance," *Physical Review Letters*, vol. 85, no. 22, pp. 4652–4655, 2000.

[122] S. P. Hegarty, G. Huyet, J. G. McInerney, and K. D. Choquette, "Pattern formation in the transverse section of a laser with a large fresnel number," *Physical Review Letters*, vol. 82, no. 7, pp. 1434–1437, 1999.

[123] I. V. Babushkin, M. Schulz-Ruhtenberg, N. A. Loiko, K. F. Huang, and T. Ackemann, "Coupling of polarization and spatial degrees of freedom of highly divergent emission in broad-area square vertical-cavity surface-emitting lasers," *Physical Review Letters*, vol. 100, no. 21, article 213901, 2008.

[124] Z. G. Pan, S. Jiang, M. Dagenais et al., "Optical injection induced polarization bistability in vertical-cavity surface-emitting lasers," *Applied Physics Letters*, vol. 63, no. 22, pp. 2999–3001, 1993.

[125] P. Besnard, M. L. Charès, G. Stéphan, and F. Robert, "Switching between polarized modes of a verticalcavity surface-emitting laser by isotropic optical feedback," *Journal of the Optical Society of America B*, vol. 16, no. 7, pp. 1059–1063, 1999.

[126] M. Giudici, S. Balle, T. Ackemann, S. Barland, and J. R. Tredicce, "Polarization dynamics in vertical-cavity surface-emitting lasers with optical feedback: experiment and model," *Journal of the Optical Society of America B*, vol. 16, no. 11, pp. 2114–2123, 1999.

[127] B. S. Ryvkin, K. Panajotov, E. A. Avrutin, I. Veretennicoff, and H. Thienpont, "Optical-injection-induced polarization switching in polarization-bistable vertical-cavity surface-emitting lasers," *Journal of Applied Physics*, vol. 96, no. 11, pp. 6002–6007, 2004.

[128] I. Gatare, M. Sciamanna, M. Nizette, and K. Panajotov, "Bifurcation to polarization switching and locking in vertical-cavity surface-emitting lasers with optical injection," *Physical Review A*, vol. 76, no. 3, article 031803, 2007.

[129] H. Kawaguchi, "Polarization-bistable vertical-cavity surface-emitting lasers: application for optical bit memory," *Opto-Electronics Review*, vol. 17, no. 4, pp. 265–274, 2009.

[130] V. J. Sánchez-Morcillo, I. Pérez-Arjona, F. Silva, G. J. de Valcárcel, and E. Roldán, "Vectorial Kerr-cavity solitons," *Optics Letters*, vol. 25, no. 13, pp. 957–959, 2000.

[131] X. Hachair, G. Tissoni, H. Thienpont, and K. Panajotov, "Linearly polarized bistable localized structure in medium-size vertical-cavity surface-emitting lasers," *Physical Review A*, vol. 79, no. 1, article 011801, 2009.

[132] F. W. Wise, "Generation of light bullets," *Physicss*, vol. 3, p. 107, 2010.

[133] S. Minardi, F. Eilenberger, Y. V. Kartashov et al., "Three-dimensional light bullets in arrays of waveguides," *Physical Review Letters*, vol. 105, no. 26, article 263901, 2010.

[134] H. C. Gurgov and O. Cohen, "Spatiotemporal pulse-train solitons," *Optics Express*, vol. 17, no. 9, pp. 7052–7058, 2009.

[135] B. A. Malomed, D. Mihalache, F. Wise, and L. Torner, "Spatiotemporal optical solitons," *Journal of Optics B*, vol. 7, no. 5, pp. R53–R72, 2005.

[136] F. Wise and P. Di Trapani, "Spatiotemporal solitons," *Optics and Photonics News*, vol. 13, no. 2, pp. 28–32, 2002.

[137] Y. Silberberg, "Collapse of optical pulse," *Optics Letters*, vol. 15, pp. 1282–1284, 1990.

[138] M. O. Williams, C. W. McGrath, and J. N. Kutz, "Light-bullet routing and control with planar waveguide arrays," *Optics Express*, vol. 18, no. 11, pp. 11671–11682, 2010.

[139] N. N. Rozanov, "On solitonlike optical structures on nonlinear optical media with gain," *Optics and Spectroscopy*, vol. 76, no. 4, pp. 555–557, 1994.

[140] N. A. Veretenov, N. N. Rosanov, and S. V. Fedorov, "Motion of complexes of 3D-laser solitons," *Optical and Quantum Electronics*, vol. 40, no. 2–4, pp. 253–262, 2008.

[141] M. Brambilla, T. Maggipinto, G. Patera, and L. Columbo, "Cavity light bullets: three-dimensional localized structures in a nonlinear optical resonator," *Physical Review Letters*, vol. 93, no. 20, article 203901, 2004.

[142] M. Brambilla, L. Columbo, and T. Maggipinto, "Three-dimensional self-organized patterns in the field profile of a ring cavity resonator," *Journal of Optics B*, vol. 6, no. 5, pp. S197–S204, 2004.

[143] S. D. Jenkins, F. Prati, L. A. Lugiato, L. Columbo, and M. Brambilla, "Cavity light bullets in a dispersive Kerr medium," *Physical Review A*, vol. 80, no. 3, Article ID 033832, 2009.

[144] L. Columbo, I. M. Perrini, T. Maggipinto, and M. Brambilla, "3D self-organized patterns in the field profile of a semiconductor resonator," *New Journal of Physics*, vol. 8, p. 312, 2006.

[145] L. Columbo, F. Prati, M. Brambilla, and T. Maggipinto, "Self-pulsing localized structures in a laser with saturable absorber," *European Physical Journal D*, vol. 59, no. 1, pp. 115–120, 2010.

[146] F. Lederer and W. Biehlig, "Bright solitons and light bullets in semiconductor waveguides," *Electronics Letters*, vol. 30, no. 22, pp. 1871–1872, 1994.

[147] A. A. Sukhorukov and Y. S. Kivshar, "Slow-light optical bullets in arrays of nonlinear Bragg-grating waveguides," *Physical Review Letters*, vol. 97, no. 23, article 233901, 2006.

[148] M. O. Williams and J. N. Kutz, "Spatial mode-locking of light bullets in planar waveguide arrays," *Optics Express*, vol. 17, no. 20, pp. 18320–18329, 2009.

[149] M. Blaauboer, G. Kurizki, and B. A. Malomed, "Spatiotemporally localized solitons in resonantly absorbing Bragg reflectors," *Physical Review E*, vol. 62, no. 1, pp. R57–R59, 2000.

[150] X. Hachair, S. Barbay, T. Elsass, I. Sagnes, and R. Kuszelewicz, "Transverse spatial structure of a high fresnel number vertical external cavity surface emitting laser," *Optics Express*, vol. 16, no. 13, pp. 9519–9527, 2008.

[151] T. Ackemann, N. Radwell, and R. Jäger, "Optically controllable microlasers and 3D light confinement based on cavity solitons in vertical-cavity devices," in *Proceedings of the 2nd IEEE/LEOS Winter Topicals (WTM '09)*, pp. 136–137, 2009.

[152] T. Ackemann, N. Radwell, C. Mcintyre, G. L. Oppo, and W. J. Firth, "Self pulsing solitons: a base for optically controllable pulse trains in photonic networks?" in *Proceedings of the 12th International Conference on Transparent Optical Networks (ICTON '10)*, pp. 1–4, 2010.

[153] A. J. Scroggie, W. J. Firth, and G. L. Oppo, "Cavity-soliton laser with frequency-selective feedback," *Physical Review A*, vol. 80, no. 1, article 013829, 2009.

[154] C. Weisbuch, M. Nishioka, A. Ishikawa, and Y. Arakawa, "Observation of the coupled exciton-photon mode splitting in a semiconductor quantum microcavity," *Physical Review Letters*, vol. 69, no. 23, pp. 3314–3317, 1992.

[155] H. M. Gibbs, G. Khitrova, and S. W. Koch, "Exciton-polariton light-semiconductor coupling effects," *Nature Photonics*, vol. 5, p. 273, 2011.

[156] G. Khitrova, H. M. Gibbs, F. Jahnke, M. Kira, and S. W. Koch, "Nonlinear optics of normal-mode-coupling semiconductor microcavities," *Reviews of Modern Physics*, vol. 71, no. 5, pp. 1591–1639, 1999.

[157] A. Amo, D. Sanvitto, F. P. Laussy et al., "Collective fluid dynamics of a polariton condensate in a semiconductor microcavity," *Nature*, vol. 457, no. 7227, pp. 291–295, 2009.

[158] J. Kasprzak, M. Richard, S. Kundermann et al., "Bose-Einstein condensation of exciton polaritons," *Nature*, vol. 443, no. 7110, pp. 409–414, 2006.

[159] S. Christopoulos, G. B. H. von Högersthal, A. J. D. Grundy et al., "Room-temperature polariton lasing in semiconductor microcavities," *Physical Review Letters*, vol. 98, no. 12, article 126405, 2007.

[160] P. G. Savvidis, J. J. Baumberg, R. M. Stevenson, M. S. Skolnick, D. M. Whittaker, and J. S. Roberts, "Angle-resonant stimulated polariton amplifier," *Physical Review Letters*, vol. 84, no. 7, pp. 1547–1550, 2000.

[161] A. Baas, J. P. Karr, H. Eleuch, and E. Giacobino, "Optical bistability in semiconductor microcavities," *Physical Review A*, vol. 69, no. 2, pp. 238091–238098, 2004.

[162] A. Baas, J. P. Karr, M. Romanelli, A. Bramati, and E. Giacobino, "Optical bistability in semiconductor microcavities in the nondegenerate parametric oscillation regime: analogy with the optical parametric oscillator," *Physical Review B*, vol. 70, no. 16, Article ID 161307, pp. 1–4, 2004.

[163] A. Tredicucci, Y. Chen, V. Pellegrini, M. Börger, and F. Bassani, "Optical bistability of semiconductor microcavities in the strong-coupling regime," *Physical Review A*, vol. 54, no. 4, pp. 3493–3498, 1996.

[164] M. Gurioli, L. Cavigli, G. Khitrova, and H. M. Gibbs, "Bistable optical response in quantum well semiconductor microcavity," *Semiconductor Science and Technology*, vol. 19, no. 4, pp. S345–S347, 2004.

[165] L. Cavigli and M. Gurioli, "Optical bistability and laserlike emission in a semiconductor microcavity," *Physical Review B*, vol. 71, no. 3, Article ID 035317, pp. 1–7, 2005.

[166] D. Bajoni, E. Semenova, A. Lemaître et al., "Optical bistability in a GaAs-based polariton diode," *Physical Review Letters*, vol. 101, no. 26, article 266402, 2008.

[167] Y. Larionova, W. Stolz, and C. O. Weiss, "Optical bistability and spatial resonator solitons based on exciton-polariton nonlinearity," *Optics Letters*, vol. 33, no. 4, pp. 321–323, 2008.

[168] D. Bajoni, P. Senellart, E. Wertz et al., "Polariton laser using single micropillar GaAs-GaAlAs semiconductor cavities," *Physical Review Letters*, vol. 100, no. 4, article 047401, 2008.

[169] A. Amo, T. C. H. Liew, C. Adrados et al., "Exciton-polariton spin switches," *Nature Photonics*, vol. 4, no. 6, pp. 361–366, 2010.

[170] O. A. Egorov, A. V. Gorbach, F. Lederer, and D. V. Skryabin, "Two-dimensional localization of exciton polaritons in microcavities," *Physical Review Letters*, vol. 105, no. 7, article 073903, 2010.

[171] A. V. Yulin, O. A. Egorov, F. Lederer, and D. V. Skryabin, "Dark polariton solitons in semiconductor microcavities," *Physical Review A*, vol. 78, no. 6, article 061801, 2008.

[172] O. A. Egorov, D. V. Skryabin, A. V. Yulin, and F. Lederer, "Bright cavity polariton solitons," *Physical Review Letters*, vol. 102, no. 15, article 153904, 2009.

[173] W. L. Zhang and S. F. Yu, "Vectorial polariton solitons in semiconductor microcavities," *Optics Express*, vol. 18, no. 20, pp. 21219–21224, 2010.

[174] O. A. Egorov, D. V. Skryabin, and F. Lederer, "Polariton solitons due to saturation of the exciton-photon coupling," *Physical Review B*, vol. 82, no. 16, article 165326, 2010.